



**HAL**  
open science

# Dynamical analysis and optimization of a generalized resource allocation model of microbial growth

Agustín Gabriel Yabo, Jean-Baptiste Caillau, Jean-Luc Gouzé, Hidde de Jong, Francis Mairet

► **To cite this version:**

Agustín Gabriel Yabo, Jean-Baptiste Caillau, Jean-Luc Gouzé, Hidde de Jong, Francis Mairet. Dynamical analysis and optimization of a generalized resource allocation model of microbial growth. SIAM Journal on Applied Dynamical Systems, 2022, 21 (1), pp.137-165. 10.1137/21M141097X . hal-03251044v1

**HAL Id: hal-03251044**

**<https://inria.hal.science/hal-03251044v1>**

Submitted on 5 Jun 2021 (v1), last revised 9 Jan 2023 (v2)

**HAL** is a multi-disciplinary open access archive for the deposit and dissemination of scientific research documents, whether they are published or not. The documents may come from teaching and research institutions in France or abroad, or from public or private research centers.

L'archive ouverte pluridisciplinaire **HAL**, est destinée au dépôt et à la diffusion de documents scientifiques de niveau recherche, publiés ou non, émanant des établissements d'enseignement et de recherche français ou étrangers, des laboratoires publics ou privés.



Distributed under a Creative Commons Attribution 4.0 International License

# Dynamical analysis and optimization of a generalized resource allocation model of microbial growth\*

Agustín Gabriel Yabo<sup>†</sup>, Jean-Baptiste Caillau<sup>‡</sup>, Jean-Luc Gouzé<sup>†</sup>, Hidde de Jong<sup>§</sup>, and Francis Mairet<sup>¶</sup>

**Abstract.** Gaining a better comprehension of the growth of microorganisms is a major scientific challenge, which has often been approached from a resource allocation perspective. Simple mathematical self-replicator models based on resource allocation principles have been surprisingly effective in accounting for experimental observations of the growth of microorganisms. Previous work, using a three-variable resource allocation model, predicted an optimal resource allocation scheme for the adaptation of microbial cells to a sudden nutrient change in the environment. We here propose an extended version of this model considering also proteins responsible for basic housekeeping functions, and we study their impact on predicted optimal strategies for resource allocation following changes in the environment. A full dynamical analysis of the system shows there is a single globally attractive equilibrium, which can be related to steady-state growth conditions of bacteria observed in experiments. We then explore the optimal allocation strategies using optimization and optimal control theory. We show that the solutions to this dynamical problem have a complicated structure that includes a second-order singular arc given in feedback form, and characterized by i) Fuller's phenomenon, and ii) the turnpike effect, producing a very particular asymptotic behaviour towards the solution of the static optimization problem. Our work thus provides a generalized perspective on the analysis of microbial growth by means of simple self-replicator models.

**Key words.** systems biology, bacterial growth laws, resource allocation, nutritional shifts, optimal control, turnpike

**AMS subject classifications.** 37N25, 49K15, 92C42

**1. Introduction.** The growth of microorganisms is a paradigm example of self-replication in Nature. Microbial cells are capable of transforming nutrients from the environment into new microbial cells astonishingly fast and in a highly reproducible manner [1]. The biochemical reaction network underlying microbial growth has evolved under the pressure of natural selection, a process that has retained changes in the network structure and dynamics increasing fitness, i.e., favoring the ability of the cells to proliferate in their environment. Gaining a better comprehension of the growth of microorganisms in the context of evolution is a major scientific challenge [2], and the ability to externally control growth is critical for a wide range of applications, such as in combating antibiotics resistance, food preservation, and biofuel

---

\*Submitted to the editors 8th April 2021.

**Funding:** This work was partially supported by ANR project Maximic (ANR-17-CE40-0024-01), Inria IPL Cosy and Labex SIGNALIFE (ANR-11-LABX-0028-01). We acknowledge the support of the FMJH Program PGMO and the support to this program from EDF-THALES-ORANGE.

<sup>†</sup>Université Côte d'Azur, Inria, INRAE, CNRS, Sorbonne Université, Biocore Team, Sophia Antipolis, France ([agustin.yabo@inria.fr](mailto:agustin.yabo@inria.fr), [www.agustinyabo.com.ar](http://www.agustinyabo.com.ar))

<sup>‡</sup>Université Côte d'Azur, CNRS, Inria, LJAD, France ([jean-baptiste.caillau@univ-cotedazur.fr](mailto:jean-baptiste.caillau@univ-cotedazur.fr))

<sup>§</sup>Université Grenoble Alpes, Inria, 38000 Grenoble, France ([hidde.de-jong@inria.fr](mailto:hidde.de-jong@inria.fr))

<sup>¶</sup>Ifremer, Physiology and Biotechnology of Algae laboratory, rue de l'Île d'Yeu, 44311 Nantes, France ([francis.mairet@ifremer.fr](mailto:francis.mairet@ifremer.fr))

34 production [3, 4, 5].

35 A fruitful perspective on microbial growth is to view it as a resource allocation problem  
36 [6]. Microorganisms must assign their available resources to different cellular functions, in-  
37 cluding the uptake and conversion of nutrients into molecular building blocks of proteins and  
38 other macromolecules (metabolism), the synthesis of proteins and other macromolecules from  
39 these building blocks (gene expression), and the detection of changes in the environment and  
40 the preparation of adequate responses (signalling and regulation). It is often assumed that  
41 microorganisms have evolved resource allocation strategies so as to maximize their growth  
42 rate, as this would allow them to outgrow competing species.

43 Simple mathematical models based on resource allocation principles have been surpris-  
44 ingly effective in accounting for experimental observations of the growth and physiology of  
45 microorganisms [6, 7, 8, 9, 10, 11, 12]. Instead of providing a detailed description of the en-  
46 tire biochemical reaction network, these models include a limited number of macroreactions  
47 responsible for the main growth-related functions of the cell. The models usually take the  
48 form of nonlinear ODE systems, typically 3-10 equations with parameters obtained from the  
49 experimental literature or estimated from published data. The models have been instrumental  
50 in explaining a number of steady-state relations between the growth rate and the cellular com-  
51 position, in particular the concentration of ribosomes, protein complexes that are responsible  
52 for the synthesis of new proteins [8, 6, 13, 10, 14]. Moreover, they have brought out a trade-off  
53 between the rate and yield of alternative metabolic pathways that produce energy-carrying  
54 molecules, necessary for driving forward many cellular reactions, such as those involved in the  
55 synthesis of proteins and other macromolecules [8, 15, 16].

56 In previous work, using a three-variable resource allocation model, it was possible to  
57 predict an optimal resource allocation scheme for the response of microbial cells to a sudden  
58 nutrient change in the environment [10]. The prediction was based on the Infinite Horizon  
59 Maximum Principle, a generalization of the well-known PMP (Pontrjagin Maximum Principle)  
60 [17, 18]. A feedback control strategy inspired by a known regulatory mechanism for growth  
61 control in the bacterial cell was shown to give a quasi-optimal approximation of the optimal  
62 solution. Strategies for optimal control were also explored for an extension of the model,  
63 inspired by recent experimental work [19], which comprises a pathway for the production  
64 of a metabolite of biotechnical interest as well as an external signal allowing growth to be  
65 switched off [20, 21, 22, 23]. We showed by a combination of analytical and computational  
66 means that the optimal solution for the targeted metabolite production problem consists of  
67 a phase of growth maximization followed by a phase of product maximization, in agreement  
68 with strategies proposed in metabolic engineering.

69 The resource allocation model that lies at the basis of the above-mentioned work has  
70 a number of limitations though. First, the biomass of the cell was assumed to consist of  
71 two classes of proteins, enzymes catalyzing metabolic reactions and ribosomes responsible for  
72 protein synthesis, whose relative proportions vary with the growth rate. However, experi-  
73 mental data show that a large fraction of the total protein contents of the cell is growth  
74 rate-independent [24]. This suggests the introduction of a third protein category, dedicated  
75 mainly to basic housekeeping functions of the cell. The proportion of these proteins is in-  
76 dependent of the growth rate and thus constrains the variations in the other two, growth  
77 rate-dependent categories [6, 13]. Second, the concentration of ribosomes and enzymes, the

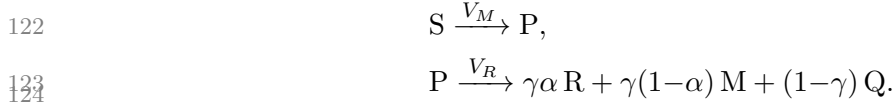
78 two protein categories included in the original model, have both a growth rate-dependent and  
79 a growth rate-independent component [6, 24]. This implies that the protein synthesis rate,  
80 and thus the growth rate, does not depend on the total ribosome concentration, as in the  
81 original model, but only on its growth rate-dependent fraction [13].

82 In the present manuscript, we revise the above modeling assumptions and study their  
83 impact on predicted optimal strategies for resource allocation following changes in the envi-  
84 ronment of different nature (i.e. changes in the nutrient concentration or stress responses).  
85 This leads to a number of interesting problems in mathematical analysis and control, which  
86 are approached using tools from dynamical systems analysis and optimal control theory. A  
87 full dynamical analysis of the system shows there is a single globally attractive equilibrium,  
88 which can be related to steady-state growth conditions of bacteria observed in experiments.  
89 In spite of the simplicity of the presented model, the solutions of the associated biomass maxi-  
90 mization problems exhibit quite interesting features. Notably, the second-order singular arc is  
91 characterized by a) the Fuller’s phenomenon in its junctions, yielding an infinite set of switch-  
92 ing points in a finite time window, and b) the turnpike effect, which produces very particular  
93 asymptotic behaviors towards the solution of the static optimization problem. In particular,  
94 we provide a full description of such singular arc in terms of the state, as well as an explicit  
95 proof of the presence of the turnpike effect along it. While the model assumptions are more  
96 realistic, the predicted (optimal) control dynamics does not change much qualitatively, yet  
97 offers a more general perspective of the biological problem. Indeed, the proposed model can  
98 serve as a generalization of the previous model, where the absence of growth-rate independent  
99 proteins yields a singular arc that is exactly equal to the solution of the static optimization  
100 problem.

101 In Section 2, we describe the model used in this study, followed by a global dynamical  
102 analysis of the model in Section 3. In Section 4, we perform a calibration from literature data  
103 using the model’s equilibrium of interest under an optimal steady-state allocation parameter,  
104 and in Section 5 we formulate an optimal control problem and prove properties of the optimal  
105 solutions. In section 6, we show that the general analysis can be applied to two different cases  
106 of environmental changes related to nutrient shifts and stress responses.

107 **2. Model definition.** We define a self-replicator system composed of the mass of precur-  
108 sor metabolites P, the gene expression machinery R (ribosomes, RNA polymerase...) and  
109 the metabolic machinery M (enzymes, transporters...), as shown in Figure 1. Essentially, the  
110 ribosomal proteins R are responsible for the fabrication of new proteins, and the metabolic  
111 proteins M are in charge of the uptake of nutrients for building precursor metabolites P. Fol-  
112 lowing Scott *et al.* [6], we also introduce a class Q of proteins whose functions fall outside the  
113 range of tasks performed by M and R. This sector comprises mainly growth rate-independent  
114 proteins such as housekeeping proteins responsible for the maintenance of certain basic cellular  
115 functions. Needless to say, the synthesis of Q proteins draws resources from the pathways to  
116 M and R, and consequently imposes an upper bound on the fraction of the cell dedicated to  
117 self-replication and nutrient uptake. This constraint appears in the model through a constant  
118  $\gamma \in [0, 1]$ , and it indicates the proportion in which the precursors are distributed across these  
119 sectors—that is, the maximum fraction of the protein synthesis rate available for making ri-  
120 bosomes and metabolic enzymes. The overall allocation process can be represented by the

121 biochemical macroreactions



The first reaction is catalyzed<sup>1</sup> by M and describes the transformation of external substrate

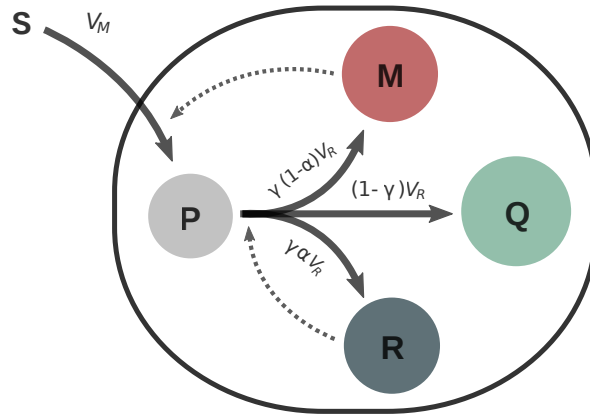


Figure 1: Coarse-grained self-replicator model. The external substrate  $S$  is consumed by bacteria and transformed into precursor metabolites  $P$  by the metabolic machinery  $M$ . These precursors are used to produce macromolecules of classes  $R$ ,  $M$  and  $Q$ ; with proportions  $\gamma\alpha$ ,  $\gamma(1-\alpha)$ , and  $1-\gamma$ , respectively. Solid lines indicate the macroreactions with their respective synthesis rates, and dashed lines denote a catalytic effect.

125

126  $S$  into precursor metabolites  $P$  at a rate  $V_M$ . The second reaction represents the conversion  
 127 of precursors into macromolecules  $R$ ,  $M$ , and  $Q$  and is catalyzed by  $R$ , at a rate  $V_R$ . The  
 128 natural resource allocation strategy is modeled through the parameter  $\alpha \in [0, 1]$ . Thus, the  
 129 proportion of the total synthesis rate of proteins dedicated to the gene expression machinery  
 130  $R$  is  $\gamma\alpha$ , while that of the metabolic machinery  $M$  is  $\gamma(1-\alpha)$ . In particular, the allocation  
 131 parameter does not influence the synthesis rate of  $Q$ , with constant proportion  $1-\gamma$ , as the  
 132 synthesis of proteins in this class is auto-regulated through mechanisms not relevant in this  
 133 study.

---

<sup>1</sup>In this context, protein  $A$  *catalyzes* reaction  $B$  means that the rate of reaction  $B$  is proportional to the concentration of  $A$  in the cell, but the reaction itself does not consume  $A$ .

134 **2.1. Self-replicator system.** Generalizing upon Giordano *et al.* [10], a mass balance  
 135 analysis yields the dynamical system

$$136 \quad \begin{cases} \dot{P} = V_M - V_R, \\ \dot{R} = \gamma\alpha V_R, \\ \dot{M} = \gamma(1 - \alpha)V_R, \\ \dot{Q} = (1 - \gamma)V_R. \end{cases}$$

137

138 where mass quantities  $P$ ,  $M$ ,  $R$  and  $Q$  are described in grams, the synthesis rates  $V_M$  and  
 139  $V_R$  in grams per hour, and  $\alpha$  is the dimensionless allocation parameter. In what follows, we  
 140 will assume that the proteins of classes  $R$ ,  $M$  and  $Q$  are responsible for most of the bacterial  
 141 mass [1], and so we define the bacterial volume  $\mathcal{V}$  [L] as

$$142 \quad (2.1) \quad \mathcal{V} = \beta(R + M + Q),$$

143

144 where  $\beta$  corresponds to a density constant relating mass and bacterial volume [25], such that  
 145 the total biomass in grams is given by  $\mathcal{V}/\beta$ . The above assumption implies that the mass of  
 146 precursor metabolites represents a negligible fraction of the total biomass, (in other words,  
 147  $P \ll \mathcal{V}/\beta$ ). We define the intracellular concentrations measured in grams per liter as

$$148 \quad (2.2) \quad p_{\mathcal{V}} \doteq \frac{P}{\mathcal{V}}, \quad r_{\mathcal{V}} \doteq \frac{R}{\mathcal{V}}, \quad m_{\mathcal{V}} \doteq \frac{M}{\mathcal{V}}, \quad q_{\mathcal{V}} \doteq \frac{Q}{\mathcal{V}}.$$

149

150 Using (2.1) and (2.2), we to obtain the relation

$$151 \quad (2.3) \quad r_{\mathcal{V}} + m_{\mathcal{V}} + q_{\mathcal{V}} = \frac{1}{\beta}.$$

152

153 We also define the rates of mass flow per unit volume, which we assume to be functions of the  
 154 available concentrations, as

$$155 \quad v_M(s, m_{\mathcal{V}}) \doteq \frac{V_M}{\mathcal{V}}, \quad v_R(p_{\mathcal{V}}, r_{\mathcal{V}}) \doteq \frac{V_R}{\mathcal{V}}.$$

156

157 where  $s$  corresponds to the extracellular concentration of substrate measured in grams per  
 158 litre. The growth rate of the bacterial population is defined as the relative change of the  
 159 bacterial volume

$$160 \quad \mu \doteq \frac{\dot{\mathcal{V}}}{\mathcal{V}} = \frac{\beta V_R}{\mathcal{V}} = \beta v_R(p_{\mathcal{V}}, r_{\mathcal{V}}).$$

161

162 We write the system in terms of the concentrations as

$$163 \quad \begin{cases} \dot{p}_{\mathcal{V}} = v_M(s, m_{\mathcal{V}}) - (1 + \beta p_{\mathcal{V}})v_R(p_{\mathcal{V}}, r_{\mathcal{V}}), \\ \dot{r}_{\mathcal{V}} = (\gamma\alpha - \beta r_{\mathcal{V}})v_R(p_{\mathcal{V}}, r_{\mathcal{V}}), \\ \dot{m}_{\mathcal{V}} = (\gamma(1 - \alpha) - \beta m_{\mathcal{V}})v_R(p_{\mathcal{V}}, r_{\mathcal{V}}), \\ \dot{q}_{\mathcal{V}} = ((1 - \gamma) - \beta q_{\mathcal{V}})v_R(p_{\mathcal{V}}, r_{\mathcal{V}}), \\ \dot{\mathcal{V}} = \beta v_R(p_{\mathcal{V}}, r_{\mathcal{V}})\mathcal{V}. \end{cases}$$

164

165 **2.2. Kinetic definition.** We define the kinetics of the reaction system by taking into  
166 account that a minimal concentration of ribosomal proteins  $r_{\mathcal{V},\min} \in (0, \gamma/\beta)$  is required for  
167 protein synthesis to take place. In other words, a part of the bacterial volume is occupied  
168 by ribosomal proteins which do not directly contribute to growth [13]. Such behavior can be  
169 modeled as

$$170 \quad v_R(p_{\mathcal{V}}, r_{\mathcal{V}}) \doteq w_R(p_{\mathcal{V}}) (r_{\mathcal{V}} - r_{\mathcal{V},\min})^+, \quad \text{with } (r_{\mathcal{V}} - r_{\min})^+ = \begin{cases} r_{\mathcal{V}} - r_{\mathcal{V},\min} & \text{if } r_{\mathcal{V}} \geq r_{\mathcal{V},\min}, \\ 0 & \text{if } r_{\mathcal{V}} < r_{\mathcal{V},\min}. \end{cases}$$

171

172 Later on, we will see that there is no need to define  $v_R(p_{\mathcal{V}}, r_{\mathcal{V}})$  for  $r_{\mathcal{V}} < r_{\mathcal{V},\min}$  if the initial  
173 conditions lie in a particular region of the state space. The rate of nutrient uptake is defined  
174 as

$$175 \quad v_M(s, m_{\mathcal{V}}) \doteq w_M(s) m_{\mathcal{V}}.$$

176

177 We will make the following assumption for functions  $w_R(p_{\mathcal{V}})$  and  $w_M(s)$ .

- 178 *Hypothesis 2.1.* Function  $w_i(x) : \mathbb{R}_+ \rightarrow \mathbb{R}_+$  is
- 179 • Continuously differentiable w.r.t.  $x$ ,
  - 180 • Null at the origin:  $w_i(0) = 0$ ,
  - 181 • Strictly monotonically increasing:  $w_i'(x) > 0, \forall x \geq 0$ ,
  - 182 • Strictly concave downwards:  $w_i''(x) < 0, \forall x \geq 0$ ,
  - 183 • Upper bounded:  $\lim_{x \rightarrow \infty} w_i(x) = k_i > 0$ .

184 The classical Michaelis-Menten kinetics satisfies Hypothesis 2.1. While most of the math-  
185 ematical results are based on this general definition, for the calibration of the model and  
186 numerical simulations, we will resort to the particular case where the functions are defined as

$$187 \quad (2.4) \quad w_R(p_{\mathcal{V}}) \doteq k_R \frac{p_{\mathcal{V}}}{K_R + p_{\mathcal{V}}}, \quad w_M(s) \doteq k_M \frac{s}{K_S + s},$$

188

189 where  $k_R$  and  $k_M$  are the maximal reaction rates in  $\text{h}^{-1}$ , and  $K_M$  and  $K_R$  are the half-  
190 saturation constants of the synthesis rates in  $\text{g L}^{-1}$ . For the general case introduced in  
191 Hypothesis 2.1 we will define

$$192 \quad k_R \doteq \lim_{p_{\mathcal{V}} \rightarrow \infty} w_R(p_{\mathcal{V}}).$$

193

194 **2.3. Constant environmental conditions.** We assume that the availability of the sub-  
 195 strate in the medium is constant over the time-window analyzed. The latter can be modeled  
 196 by setting  $s$  constant, and thus removing the dynamics of  $s$  from the system.

197 *Hypothesis 2.2.* The flow of substrate can be expressed as  $w_M(s) = e_M$  with  $e_M > 0$   
 198 constant.

199 Using this assumption, the dynamical equation of  $p_V$  becomes

$$200 \quad \dot{p}_V = e_M m_V - (1 + \beta p_V) w_R(p_V) (r_V - r_{V,\min})^+.$$

202 The constant  $e_M$  models the substrate availability of the medium, but it is also related to  
 203 the quality of the nutrient and the efficiency of the macroreaction that produces precursor  
 204 metabolites.

205 **2.4. Mass fraction formulation and non-dimensionalization.** We define mass fractions  
 206 of the total bacterial mass as

$$207 \quad p \doteq \beta p_V, \quad r \doteq \beta r_V, \quad r_{\min} \doteq \beta r_{V,\min}, \quad m \doteq \beta m_V, \quad q \doteq \beta q_V,$$

209 which, replacing in (2.3), yields the relation

$$210 \quad (2.5) \quad r + m + q = 1.$$

212 We also define the non-dimensional time variable  $\hat{t} \doteq k_R t$ , and the non-dimensional growth  
 213 rate

$$214 \quad (2.6) \quad \hat{\mu}(p, r) \doteq \frac{\mu(p_V, r_V)}{k_R} = \hat{w}_R(p) (r - r_{\min}),$$

216 with  $\hat{w}_R(p) : \mathbb{R}_+ \rightarrow [0, 1)$  defined as  $\hat{w}_R(p) \doteq w_R(p_V)/k_R$ , and  $E_M \doteq e_M/k_R$ . For the sake of  
 217 simplicity, let us drop all hats from the current notation. Then, the model becomes

$$218 \quad (S) \quad \begin{cases} \dot{p} = E_M m - (p + 1) w_R(p) (r - r_{\min})^+, \\ \dot{r} = (\gamma \alpha - r) w_R(p) (r - r_{\min})^+, \\ \dot{m} = (\gamma(1 - \alpha) - m) w_R(p) (r - r_{\min})^+, \\ \dot{\mathcal{V}} = w_R(p) (r - r_{\min})^+ \mathcal{V}, \\ m + r \leq 1, \end{cases}$$

219  
 220 where  $q$  has been removed since it can be expressed in terms of the other concentrations  
 221 through (2.5); and the constraint  $m + r \leq 1$  is required to comply with  $q \geq 0$ . The model  
 222 differs from that of Giordano *et al.* by the addition of the category of housekeeping proteins  
 223 ( $q$ ) and a minimum concentration of ribosomes for protein synthesis ( $r_{\min}$ ). In what follows,  
 224 we will systematically investigate how these differences affect the asymptotic behavior and  
 225 optimal resource allocation strategies.



226 **3. Asymptotic behavior.** In the present section, we will study the asymptotic behavior  
 227 of the reduced system representing the intracellular dynamics

$$228 \quad (3.1) \quad \begin{cases} \dot{p} = E_M m - (p+1)w_R(p)(r-r_{\min})^+, \\ \dot{r} = (\gamma\alpha - r)w_R(p)(r-r_{\min})^+, \\ \dot{m} = (\gamma(1-\alpha) - m)w_R(p)(r-r_{\min})^+, \\ m+r \leq 1, \end{cases}$$

229

230 where  $\mathcal{V}$  has been removed since none of the remaining states explicitly depends on it, and  
 231 it only reaches a steady state when there is no bacterial growth (otherwise,  $\dot{\mathcal{V}} > 0$ ). We will  
 232 start by stating the invariant set of interest.

233 **Lemma 3.1.** *The set*

$$234 \quad \Gamma = \{(p, r, m) \in \mathbb{R}^3 : p \geq 0, \gamma \geq r \geq r_{\min}, \gamma \geq m \geq 0, m+r \leq 1\}$$

236 *is positively invariant by (3.1).*

237 *Proof.* This can be easily verified by evaluating the differential equations of system (3.1)  
 238 over the boundaries of  $\Gamma$ . As for the condition  $m+r \leq 1$ , we can define a variable  $z \doteq m+r$   
 239 that obeys the dynamics

$$240 \quad \dot{z} = (\gamma - z)w_R(p)(r - r_{\min})^+$$

242 which, when evaluated at  $z = 1$  yields  $\dot{z} \leq 0$ , as  $r_{\max} < 1$ , which proves its invariance.  $\blacksquare$

243 This Lemma states that  $\gamma \geq r \geq r_{\min}$  for any trajectory with initial conditions in  $\Gamma$ . As a  
 244 consequence, there is no need to define the flow  $v_R(p, r)$  for values of  $r$  under  $r_{\min}$ . The same  
 245 thing can be said for the constraint  $m+r \leq 1$ , which is valid for every trajectory starting in  
 246  $\Gamma$ . Additionally, since  $\gamma$  represents the maximal ribosomal mass fraction, we will define the  
 247 following parameter.

248 **Definition 3.2.** *The maximal ribosomal mass fraction is  $r_{\max} \doteq \gamma$ .*

249 Then, we will reduce the study of the system to this set and so, using Definition 3.2, we  
 250 redefine (3.1) as

$$251 \quad (S') \quad \begin{cases} \dot{p} = E_M m - (p+1)w_R(p)(r-r_{\min}) \\ \dot{r} = (r_{\max}\alpha - r)w_R(p)(r-r_{\min}) \\ \dot{m} = (r_{\max}(1-\alpha) - m)w_R(p)(r-r_{\min}) \end{cases}$$

252

253 where  $(r-r_{\min})^+$  has been replaced by  $r-r_{\min}$ , and the constraint  $m+r \leq 1$  has been removed.  
 254 Furthermore, we will define the minimum constant allocation parameter  $\alpha_{\min}^*$  necessary to  
 255 allow steady-state self-replication, given by

$$256 \quad \alpha_{\min}^* \doteq \frac{r_{\min}}{r_{\max}}.$$

257

258 Its importance will be analyzed throughout the current section.

### 3.1. Local stability.

**Theorem 3.3.** *System (S') has the equilibria*

- $E_1 \doteq (p^*, r^*, m^*)$ , *unique and locally stable if  $\alpha^* > \alpha_{\min}^*$ .*
- $E_2 \doteq (p, r_{\min}, 0)$ , *locally unstable if  $\alpha^* > \alpha_{\min}^*$ .*
- $E_3 \doteq (0, r, 0)$ , *locally unstable if  $r \neq r_{\min}$ .*

with

$$(3.2) \quad \begin{aligned} p^* &\doteq \left\{ p \in \mathbb{R}_+ : (p+1)w_R(p) = \frac{E_M m^*}{r^* - r_{\min}} \right\}, \\ r^* &\doteq r_{\max} \alpha^*, \\ m^* &\doteq r_{\max}(1 - \alpha^*). \end{aligned}$$

*Proof.* The general Jacobian matrix of the system (S') is

$$(3.3) \quad \begin{bmatrix} -(w_R(p) + (p+1)w'_R(p))(r - r_{\min}) & -(p+1)w_R(p) & E_M \\ (r_{\max}\alpha - r)w'_R(p)(r - r_{\min}) & (r_{\max}\alpha - 2r + r_{\min})w_R(p) & 0 \\ (r_{\max}(1 - \alpha) - m)w'_R(p)(r - r_{\min}) & (r_{\max}(1 - \alpha) - m)w_R(p) & -w_R(p)(r - r_{\min}) \end{bmatrix}.$$

We first see that, if  $\alpha^* > \alpha_{\min}^*$ , the value  $p^*$  is unique since  $(p+1)w_R(p) \in [0, \infty)$  is a monotone increasing function, and  $E_M m^*/(r^* - r_{\min}) > 0$ , so the set (3.2) yields a unique solution. For  $\alpha^* < \alpha_{\min}^*$ , the equation has no valid solution and so the equilibrium does not exist. The Jacobian (3.3) for  $E_1$  becomes

$$J_1 = \begin{bmatrix} -(w_R(p^*) + (p^*+1)w'_R(p^*))(r^* - r_{\min}) & -(p^*+1)w_R(p^*) & E_M \\ 0 & -(r^* - r_{\min})v_R(p^*) & 0 \\ 0 & 0 & -v_R(p^*)(r^* - r_{\min}) \end{bmatrix}$$

and so the local stability of the equilibrium is given by the roots of the polynomial  $\lambda = -(w_R(p^*) + (p^*+1)w'_R(p^*))(r^* - r_{\min})$ ,  $\lambda = -(p^*+1)w_R(p^*)$ , and  $\lambda = -v_R(p^*)(r^* - r_{\min})$ , which means that, if the equilibrium exists, it is locally stable. For the second equilibrium  $E_2$ , the Jacobian is

$$J_2 = \begin{bmatrix} 0 & -w_R(p) & E_M \\ 0 & (r^* - r_{\min})w_R(p) & 0 \\ 0 & r_{\max}(1 - \alpha^*)w_R(p) & 0 \end{bmatrix}$$

with characteristic polynomial

$$P_2(\lambda) = \lambda^2(\lambda - (r^* - r_{\min})w_R(p)) = 0.$$

If  $\alpha^* > \alpha_{\min}^*$ , then  $P_2(\lambda)$  has one positive eigenvalue and  $E_2$  becomes locally unstable. As for  $E_3$ , the Jacobian is

$$J_3 = \begin{bmatrix} -w'_R(0)(r - r_{\min}) & 0 & E_M \\ (r_{\max}\alpha - r)w'_R(0)(r - r_{\min}) & 0 & 0 \\ r_{\max}(1 - \alpha)w'_R(0)(r - r_{\min}) & 0 & 0 \end{bmatrix}$$

291 with characteristic polynomial

$$292 \quad P_3(\lambda) = \lambda^2 \left( \lambda + w'_R(0)(r - r_{\min}) \right) - E_M r_{\max} (1 - \alpha) w'_R(0)(r - r_{\min}) \lambda.$$

294 One root is  $\lambda = 0$ , and the two remaining roots can be found by solving the equation

$$295 \quad \lambda^2 + \lambda w'_R(0)(r - r_{\min}) - E_M r_{\max} (1 - \alpha) w'_R(0)(r - r_{\min}) = 0.$$

297 By the Routh-Hurwitz criterion, the two remaining roots are in the open left half plane if  
298 and only if  $w'_R(0)(r - r_{\min}) > 0$  and  $E_M r_{\max} (1 - \alpha) w'_R(0)(r - r_{\min}) < 0$ , which is never  
299 true. Consequently, for  $r \neq r_{\min}$ , there is at least one positive root, and so the equilibrium is  
300 unstable. ■

301 **3.2. Global behavior.** We will study the global behavior of system (S') for the initial  
302 conditions

$$303 \quad (\text{IC}) \quad p(0) > 0, \quad r(0) \in (r_{\min}, r_{\max}), \quad m(0) \in (0, r_{\max}), \quad r(0) + m(0) \leq 1.$$

305 and for a given constant allocation parameter

$$306 \quad \alpha(t) = \alpha^* \in (\alpha_{\min}^*, 1).$$

308 Under this constraint, we see that the dynamics of  $r$  and  $m$  become

$$309 \quad \dot{r} = (r^* - r)w_R(p)(r - r_{\min}), \quad \dot{m} = (m^* - m)w_R(p)(r - r_{\min}),$$

311 which means that, if  $p > 0$  and  $r > r_{\min}$ , the signs of  $\dot{r}$  and  $\dot{m}$  are given by the signs of  $r^* - r$   
312 and  $m^* - m$ , respectively (and both  $\dot{r}$  and  $\dot{m}$  are zero if  $p = 0$  or  $r = r_{\min}$ ). Then, let us  
313 divide  $\Gamma$  into the subsets

$$314 \quad \mathcal{R}^- \doteq \{(p, r, m) \in \Gamma : r \in (r_{\min}, r^*)\}, \quad \mathcal{M}^- \doteq \{(p, r, m) \in \Gamma : m \in (0, m^*)\},$$

$$315 \quad \mathcal{R}^+ \doteq \{(p, r, m) \in \Gamma : r \in (r^*, r_{\max})\}, \quad \mathcal{M}^+ \doteq \{(p, r, m) \in \Gamma : m \in (m^*, r_{\max})\},$$

316 such that  $\Gamma = \overline{\mathcal{R}^-} \cup \overline{\mathcal{R}^+} = \overline{\mathcal{M}^-} \cup \overline{\mathcal{M}^+}$ . In these sets, the following holds.

317 **Lemma 3.4.** For  $\alpha(t) = \alpha^* \in (\alpha_{\min}^*, 1)$ , the closed sets  $\overline{\mathcal{R}^-}$ ,  $\overline{\mathcal{R}^+}$ ,  $\overline{\mathcal{M}^-}$  and  $\overline{\mathcal{M}^+}$  are invariant  
318 by (S'), and

$$319 \quad \begin{cases} \dot{r} \geq 0 & \text{if } (p, r, m) \in \mathcal{R}^-, \\ \dot{r} \leq 0 & \text{if } (p, r, m) \in \mathcal{R}^+, \end{cases} \quad \begin{cases} \dot{m} \geq 0 & \text{if } (p, r, m) \in \mathcal{M}^-, \\ \dot{m} \leq 0 & \text{if } (p, r, m) \in \mathcal{M}^+. \end{cases}$$

321 Again, the invariance of the sets can be checked by evaluating the vector field over the  
322 boundaries of the sets. Now we state a first result.

323 **Proposition 3.5.** For  $\alpha(t) = \alpha^* \in (\alpha_{\min}^*, 1)$  and initial conditions (IC), system (S') has a  
324 lower bound

$$325 \quad (p, r, m) \geq (p_{\text{low}}, r_{\text{low}}, m_{\text{low}}) \text{ for all } t \geq 0,$$

327 with

$$328 \quad (3.4) \quad \begin{aligned} r_{\text{low}} &\doteq \min(r(0), r^*), & m_{\text{low}} &\doteq \min(m(0), m^*), \\ p_{\text{low}} &\doteq \left\{ p \in \mathbb{R}_+ : (p+1)w_R(p) = \frac{E_M m_{\text{low}}}{r_{\max} - r_{\min}} \right\}. \end{aligned}$$

329

330 *Proof.* For a trajectory emanating from  $\mathcal{R}^-$  (respectively,  $\mathcal{R}^+$ ), it follows that  $\dot{r} \geq 0$   
 331 (respectively,  $\dot{r} \leq 0$ ) for all  $t$  (according to Lemma 3.4), and so  $r \geq r(0)$  (respectively,  $r \geq r^*$ )  
 332 for all  $t$ . This proves that  $r \geq \min(r(0), r^*) > r_{\min}$  for all  $t$  (depending on whether the  
 333 trajectory starts in  $\mathcal{R}^-$  or  $\mathcal{R}^+$ ). Similarly, a trajectory starting in  $\mathcal{M}^-$  (respectively,  $\mathcal{M}^+$ )  
 334 meets  $\dot{m} \geq 0$  (respectively,  $\dot{m} \leq 0$ ) for all  $t$ , and so  $m \geq m(0)$  (respectively,  $m \geq m^*$ ) for all  
 335  $t$ . Then, it follows that  $m \geq \min(m(0), m^*)$  for all  $t \geq 0$ . The equation for  $p$  can thus be  
 336 lower-bounded to

$$337 \quad \dot{p} \geq E_M m_{\text{low}} - (p + 1)w_R(p)(r_{\text{max}} - r_{\text{min}}),$$

339 which means  $p \geq p_{\text{low}}$  for all  $t \geq 0$ , with  $p_{\text{low}}$  the solution of (3.4), which is unique by the  
 340 same arguments as those used in Theorem 3.3. ■

341 A lower bound on system (S') is a stronger condition than the classical persistence for bio-  
 342 logical populations, as the bound is imposed not only for  $t \rightarrow \infty$  but for the whole trajectory.  
 343 As a consequence, the growth rate never vanishes, as it meets  $\mu(p, r) \geq w_R(p_{\text{low}})(r_{\text{low}} - r_{\text{min}}) >$   
 344  $0$  for all  $t \geq 0$ . Then, the global stability of the system is straightforward.

345 **Theorem 3.6.** For  $\alpha(t) = \alpha^* \in (\alpha_{\min}^*, 1)$  and initial conditions (IC), every solution of (S')  
 346 converges to the equilibrium  $E_1$ .

347 *Proof.* Since  $p \geq p_{\text{low}} > 0$  and  $r \geq r_{\text{low}} > r_{\text{min}}$  for all  $t \geq 0$ , we have that  $\text{sign}(\dot{r}) =$   
 348  $\text{sign}(r^* - r)$  and  $\text{sign}(\dot{m}) = \text{sign}(m^* - m)$ , showing that  $r$  and  $m$  converge asymptotically to  $r^*$   
 349 and  $m^*$ , respectively. Consequently, the dynamical equation of  $p$  becomes  $\dot{p} = E_M m^* - (p +$   
 350  $1)w_R(p)(r^* - r_{\text{min}})$  and so  $\text{sign}(\dot{p}) = \text{sign}(p^* - p)$ , which means that  $p$  converges asymptotically  
 351 to the steady-state value  $p^*$ . ■

352 **Remark 3.7.** For the case over the invariant plane given by  $r(0) = r_{\text{min}}$  and  $m(0) > 0$ ,  
 353 concentrations  $m$  and  $r$  are constant along the whole trajectory, and  $p$  increases linearly with  
 354 time (as  $\dot{p} = E_M m(0)$ ). This is a degenerate case that contradicts the assumption  $p \ll 1$ , and  
 355 lacks biological relevance.

356 **3.3. Maximum steady-state growth rate.** A classical hypothesis in the literature is to  
 357 suppose bacterial populations in steady-state regimes maximize their growth rate ([10] and  
 358 references therein). We are interested in finding the static allocation strategy  $\alpha^*$  that produces  
 359 this situation. Since the only equilibrium that admits bacterial growth is  $E_1$ , we will express  
 360 the static optimization problem as

$$361 \quad \max_{\alpha^* \in [\alpha_{\min}^*, 1]} \mu(p^*, r^*),$$

363 which can be rewritten as  $\mu(p^*, r^*) = w_R(p^*)(r^* - r_{\text{min}})$ . It is possible to express  $\alpha^*$  in terms  
 364 of  $p^*$  through the relation

$$365 \quad (3.5) \quad \alpha^*(p^*) = \frac{E_M + (p^* + 1)w_R(p^*)\alpha_{\min}^*}{E_M + (p^* + 1)w_R(p^*)}.$$

367 Moreover, since the above function  $\alpha^*(p^*) : \mathbb{R}_+ \rightarrow (\alpha_{\min}^*, 1]$  is monotone decreasing, it is  
 368 possible to write the optimization problem in terms of  $p^*$  instead of  $\alpha^*$ . The growth rate in

369 terms of  $p^*$  writes

$$370 \quad (3.6) \quad w_R(p^*)(r^* - r_{\min}) = (r_{\max} - r_{\min}) \left( \frac{E_M w_R(p^*)}{E_M + (p^* + 1)w_R(p^*)} \right).$$

371

372 We differentiate w.r.t.  $p^*$  and we get the relation  $w_R(p^*)^2 = E_M w'_R(p^*)$ , which has a unique  
 373 solution since, by hypothesis,  $w_R(p)^2 \in [0, \infty)$  is a monotone increasing function, and  $w'_R(p) \in$   
 374  $[w'_R(0), 0)$  is a monotone decreasing function. Then, the condition for optimality can be  
 375 expressed as

$$376 \quad (3.7) \quad \frac{w_R(p_{\text{opt}}^*)^2}{E_M w'_R(p_{\text{opt}}^*)} = 1.$$

377

378 Thus, the optimal allocation parameter  $\alpha^*$  is obtained by replacing  $p_{\text{opt}}^*$  in (3.5), and the  
 379 maximal static growth rate can be calculated using (3.6). From (3.7), it can be seen that  $p_{\text{opt}}^*$   
 380 depends neither on  $r_{\min}$  nor on  $r_{\max}$ , suggesting that the steady-state precursor concentration  
 381 is independent of the housekeeping protein fraction  $q$  and of the growth rate-independent  
 382 ribosomal fraction. Conversely, the precursor concentration is rather determined by the en-  
 383 vironmental conditions and by the nature of the function  $w_R(p)$ . It can be proven that the  
 384 latter result is not a consequence of assumption (2.1): when considering a definition of the  
 385 bacterial volume as  $\beta(P + R + M + Q)$ , which takes into account the mass  $P$ , the optimal  
 386 precursor concentration amounts to  $p_{\text{opt}}^*/(1 + p_{\text{opt}}^*)$ .

387 In addition, from  $\dot{p} = 0$  in (S'), we get:

$$388 \quad \frac{r^* - r_{\min}}{m^*} = \frac{E_m}{(p^* + 1)w_R(p^*)}.$$

389

390 This shows that, for the optimal steady state, the concentration ratio of the active gene expres-  
 391 sion machinery over the metabolic machinery does not depend on  $r_{\max}$  either. Thus, a cellular  
 392 strategy regulating the precursor concentration and the balance between gene expression and  
 393 metabolism could lead to the optimal equilibrium, regardless of the demand for  $Q$ .

394 **4. Model calibration.** Whereas the parameter values do not affect the results above and  
 395 the optimal control analysis in the next section, they are nevertheless important for simulations  
 396 illustrating the dynamics and optimal allocation strategies of system (S'). Below, we derive  
 397 such parameters for the model bacterium *Escherichia coli*, using published sources. The  $\beta$   
 398 constant used in the definition of the bacterial volume (2.1) corresponds to the inverse of the  
 399 protein density, which is set to  $0.003 \text{ [L g}^{-1}\text{]}$  based on [10]. According to [6], the ribosomal  
 400 fraction of the proteome<sup>2</sup> can vary between 6% and 55%. In more recent studies [24], this sector  
 401 is divided into growth-rate dependent and independent fractions. The maximal growth-rate  
 402 dependent ribosomal fraction of the proteome is estimated to be 41%, and the growth rate-  
 403 independent fraction is 9%. Based on these experimental estimations, we set  $r_{\max} = 0.41 +$   
 404  $0.09 = 0.5$ . We performed further calibrations using data sets from [26, 27, 6, 24] containing  
 405 measurements of various strains of *E. coli* growing in different media. The data sets are

---

<sup>2</sup>The proteome is the total amount of protein in the cell

406 composed essentially of data points (*growth rate, RNA/protein mass ratio*) measured at steady  
 407 state. Most RNA is ribosomal RNA found overwhelmingly in ribosomes, the main constituent  
 408 of the gene expression machinery. In order to adjust the measurements to model (S'), the  
 409 observed RNA/protein ratios can be converted to mass fractions  $r$  through multiplication  
 410 with a conversion factor  $\rho = 0.76 \mu\text{g}$  of protein/ $\mu\text{g}$  of RNA [6]. As a result, we have  $n$   
 411 measurements of form  $(\tilde{\mu}_k, \tilde{r}_k)$  which are assumed to follow a linear relation [6], as seen in  
 Figure 2a. From the vertical intercept of the resulting linear regression performed using the

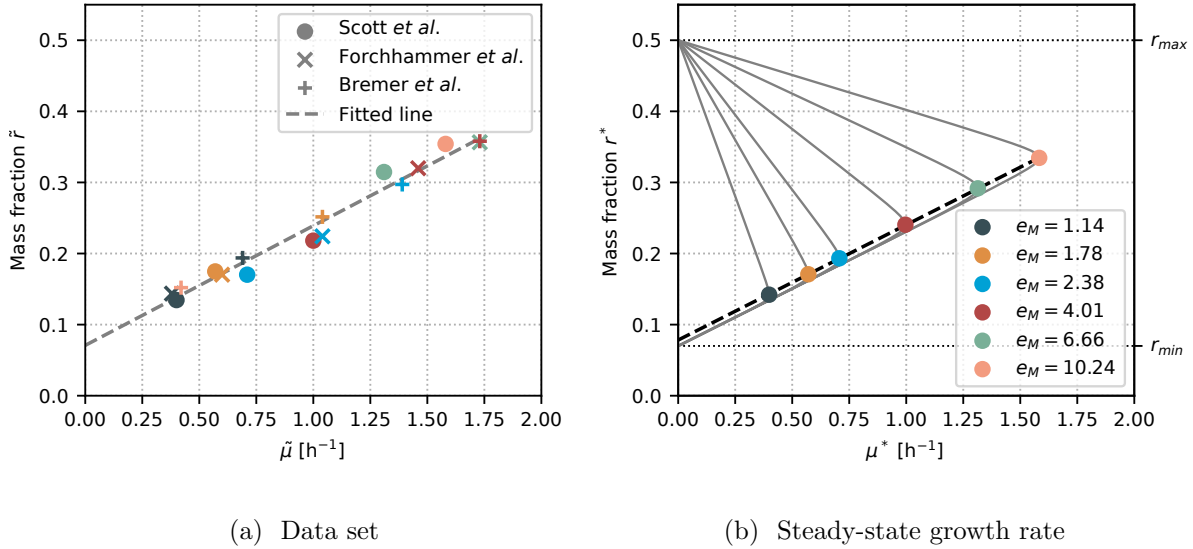


Figure 2: Experimental data from [6, 26, 27] plotted in (a) shows a linearity of  $r^2 = 0.9739$  (dashed line, fitted to data) with a vertical intercept  $r_{\min} = 0.07$  and slope  $k_R = 6.23 \text{ h}^{-1}$ . In (b), steady-state growth rate curves  $\mu^*$  are shown in terms of the mass fraction  $r^* \in (r_{\min}, r_{\max})$  for different fitted values of  $e_M$ . Each optimal pair  $(\mu_{\text{opt}}^*, r_{\text{opt}}^*)$  marked with color circles corresponds to a sample from the data set of Scott *et al.* denoted in (a) with circles of matching colors.

412 data points, we obtain  $r_{\min} = 0.07$ , in agreement with previous studies [6, 13, 24]. Each data  
 413 point, composed of an observed growth rate and its associated ribosomal mass fraction, can  
 414 be related to an optimal steady state of system (S') for a certain environmental condition  $e_M$ .  
 415 Thus, each  $k$ th pair  $(\tilde{\mu}_k, \tilde{r}_k)$  of the  $n$  measurements should yield a constant environmental  
 416 condition  $e_{M,k}$ , and all pairs should simultaneously adjust the rate constant  $k_R$ . Such fitting  
 417 can be done by resorting to the Michaelis-Menten kinetic form introduced in (2.4). Based on  
 418 [10], we fix the half-saturation constant of protein synthesis  $K_R = 1 \text{ g L}^{-1}$ . We then define  
 419 the parameter vector  $\theta = (k_R, e_{M,1}, \dots, e_{M,n})$  which is computed through a least-squares  
 420 regression problem. Using the relation (2.6), the cost function to minimize is  
 421

$$\min_{\theta \in \mathbb{R}_+^{n+1}} \sum_{k=1}^n (\tilde{\mu}_k - \mu_{\text{opt}}^*(k_R, e_{M,k}))^2 + (\tilde{r}_k - r_{\text{opt}}^*(k_R, e_{M,k}))^2,$$

424 where the non-dimensional growth rate  $\mu_{\text{opt}}^*$  is calculated using (3.6), and the optimal steady  
 425 state  $(r_{\text{opt}}^*, p_{\text{opt}}^*, m_{\text{opt}}^*)$  is expressed in terms of  $\alpha_{\text{opt}}^*$  (using Theorem 3.3) which is, at the same  
 426 time, a function of  $k_R$  and  $e_{M,k}$ . The numerical solution yields  $k_R = 6.23 \text{ h}^{-1}$ , and different  
 427 values of  $e_M$  matching different nutrients from the dataset (see Figure 2b). We can validate  
 428 these results by computing the maximal growth rate  $k_R(r_{\text{max}} - r_{\text{min}}) = 2.68 \text{ h}^{-1}$  based on  
 429 the adjusted parameters, which is a value that corresponds well with literature values of the  
 430 maximal growth rate of *E. coli* in rich media [27].

## 431 5. Optimal resource allocation.

432 **5.1. Problem definition.** In this section we formulate the dynamic optimization problem  
 433 under the hypothesis that microbial populations have evolved resource allocation strategies  
 434 enabling them to maximize their biomass in a given time window. This is represented by an  
 435 OCP (Optimal Control Problem) where the objective is to maximize the final volume at time  
 436  $T$  given by  $\mathcal{V}(T)$ . For the sake of convenience, we propose to maximize the quantity  $\log \mathcal{V}(T)$   
 437 (since  $\log$  is an increasing function) given by

$$438 \quad \log \mathcal{V}(T) = \int_0^T \mu(p, r) dt + \log \mathcal{V}(0).$$

440 As the initial condition  $\mathcal{V}(0)$  is fixed, we define the cost function

$$441 \quad J(u) \doteq \int_0^T \mu(p, r) dt = \int_0^T w_R(p)(r - r_{\text{min}}) dt.$$

443 Since  $\mathcal{V}$  appears neither in the dynamics nor in the cost function, the optimal problem will  
 444 be written considering the reduced system introduced in (S') with initial conditions given by  
 445 (IC). We write the optimal control problem

$$446 \quad (\text{OCP}) \quad \left\{ \begin{array}{l} \text{maximize} \quad J(u) = \int_0^T w_R(p)(r - r_{\text{min}}) dt \\ \text{subject to} \quad \text{dynamics (S')}, \\ \quad \quad \quad \text{initial conditions (IC)}, \\ \quad \quad \quad \alpha(\cdot) \in \mathcal{U}, \end{array} \right.$$

447  
 448 with  $\mathcal{U}$  the set of admissible controllers, which are Lebesgue measurable real-valued functions  
 449 defined on the interval  $[0, T]$  and satisfying the constraint  $\alpha(t) \in [0, 1]$ . In principle, problem  
 450 (OCP) resembles the optimal control problem proposed in [10]: the objective is to maximize  
 451 the accumulation of a certain quantity within the system during a fixed time interval  $[0, T]$   
 452 with no final state constraints. The main difference lies in the dynamics of the system, as  
 453 the introduction of the protein Q increases the system dimension by one, which yields a  
 454 more relevant (and more complex) associated OCP. We will see in following sections that the  
 455 problem raised in this work can be solved by a generalization of Giordano *et al.*'s approach.

456 **5.2. Pontrjagin Maximum Principle.** Existence of a solution for this class of OCPs is  
 457 rather trivial. Given that there are no terminal constraints, there is no controllability issue.  
 458 Moreover, the dynamics is affine in the control with the latter included in a compact and  
 459 convex set (a closed interval), and one can easily check that every finite time trajectory  
 460 remains bounded. So existence is guaranteed by Filippov's theorem [28]. Then, for an optimal  
 461 control problem (OCP) with state  $\varphi \in \mathbb{R}^n$ , Pontrjagin maximum principle (PMP) ensures that  
 462 there exist  $\lambda^0 \leq 0$  and a piecewise absolutely continuous mapping  $\lambda(\cdot) : [0, T] \rightarrow \mathbb{R}^n$ , with  
 463  $(\lambda(\cdot), \lambda^0) \neq (0, 0)$ , such that the extremal  $(\varphi, \lambda, \lambda^0, \alpha)$  satisfies the generalized Hamiltonian  
 464 system

$$465 \quad (\text{PMP}) \quad \begin{cases} \dot{\varphi} = \frac{\partial}{\partial \lambda} H(\varphi, \lambda, \lambda^0, \alpha), \\ \dot{\lambda} = -\frac{\partial}{\partial \varphi} H(\varphi, \lambda, \lambda^0, \alpha), \\ H(\varphi, \lambda, \lambda^0, \alpha) = \max_{\alpha \in [0,1]} H(\varphi, \lambda, \lambda^0, \alpha), \end{cases}$$

467 for almost every  $t \in [0, T]$ . For our particular case, we have the state vector  $\varphi \doteq (p, r, m)$  and  
 468 adjoint vector  $\lambda \doteq (\lambda_p, \lambda_r, \lambda_m)$  and the Hamiltonian given by

$$469 \quad (5.1) \quad H(\varphi, \lambda, \lambda^0, \alpha) = \lambda^0 w_R(p)(r - r_{\min}) + \langle \lambda, F(\varphi, u) \rangle,$$

471 where  $F$  represents the right-hand side of system (S'). Given that in (OCP) there is no terminal  
 472 condition on the state  $\varphi(T)$ , the transversality condition for the adjoint state is  $\lambda(T) = 0$ ,  
 473 and we can discard abnormal extremals from the analysis. In other words, any extremal  
 474  $(\varphi, \lambda, \lambda^0, \alpha)$  satisfying PMP is normal, so  $\lambda^0 \neq 0$ . Developing (5.1) yields the Hamiltonian

$$475 \quad H = \left( E_M m - (p + 1)w_R(p)(r - r_{\min}) \right) \lambda_p + (r_{\max} \alpha - r)w_R(p)(r - r_{\min}) \lambda_r \\ 476 \quad + (r_{\max}(1 - \alpha) - m)w_R(p)(r - r_{\min}) \lambda_m - \lambda^0 w_R(p)(r - r_{\min}),$$

478 and the adjoint system is

$$479 \quad (5.2) \quad \begin{cases} \dot{\lambda}_p = w_R(p)(r - r_{\min}) \lambda_p + (p + 1)w'_R(p)(r - r_{\min}) \lambda_p - (r_{\max} \alpha - r)w'_R(p)(r - r_{\min}) \lambda_r \\ \quad - (r_{\max}(1 - \alpha) - m)w'_R(p)(r - r_{\min}) \lambda_m + \lambda^0 w'_R(p)(r - r_{\min}), \\ \dot{\lambda}_r = (p + 1)w_R(p) \lambda_p + w_R(p)(r - r_{\min}) \lambda_r - (r_{\max} \alpha - r)w_R(p) \lambda_r \\ \quad - (r_{\max}(1 - \alpha) - m)w_R(p) \lambda_m + \lambda^0 w_R(p), \\ \dot{\lambda}_m = -E_M \lambda_p + w_R(p)(r - r_{\min}) \lambda_m. \end{cases}$$



481 Since the Hamiltonian is linear in the control  $\alpha$ , we rewrite it in the input-affine form  $H =$   
 482  $H_0 + \alpha H_1$  with

$$\begin{aligned}
 483 \quad H_0 &= \left( E_M m - (p+1)w_R(p)(r - r_{\min}) \right) \lambda_p - r w_R(p)(r - r_{\min}) \lambda_r \\
 484 \quad &\quad + \left( r_{\max} - m \right) w_R(p)(r - r_{\min}) \lambda_m - \lambda^0 w_R(p)(r - r_{\min}), \\
 485 \quad (5.3) \quad H_1 &= r_{\max} w_R(p)(r - r_{\min}) (\lambda_r - \lambda_m).
 \end{aligned}$$

487 The constrained optimal control  $\alpha$  should maximize the Hamiltonian, so the solution is

$$488 \quad \alpha(t) = \begin{cases} 0 & \text{if } H_1 < 0, \\ 1 & \text{if } H_1 > 0, \\ \alpha_{\text{sing}}(t) & \text{if } H_1 = 0, \end{cases}$$

490 where  $\alpha_{\text{sing}}(t)$  is called a singular control, showing that any optimal control is a concatenation  
 491 of bangs ( $\alpha = \pm 1$ ) and singular arcs, depending on the sign of the switching function  $H_1$ . As  
 492 obtained in [21, 23], a bang arc  $\alpha = 0$  (respectively  $\alpha = 1$ ) corresponds to a pure allocation  
 493 strategy where the production of  $R$  (respectively  $M$ ) is completely switched off. While a full  
 494 description of the optimal control is often difficult to obtain through PMP, there are certain  
 495 analyses that can be performed to help understand its structure. We will first see that the  
 496 final bang of the optimal control is an upper bang  $\alpha = 1$ .

497 **Lemma 5.1.** *There exists  $\epsilon$  such that the optimal control solution of (OCP) is  $\alpha(t) = 1$  for*  
 498 *the interval of time  $[T - \epsilon, T]$ .*

499 *Proof.* We define  $\lambda_z = \lambda_r - \lambda_m$ , where its dynamics can be obtained from (5.2). It can be  
 500 seen that, when evaluating its dynamics at final time, we get

$$501 \quad \dot{\lambda}_z(T) = \lambda^0 w_R(p(T)) < 0,$$

503 due to the whole adjoint state being null at final time except for  $\lambda^0$ . As  $\lambda_z(T)$  also vanishes  
 504 due to the transversality conditions, we have  $\lambda_z(T - \epsilon) > 0$  for a certain  $\epsilon$ . Then,  $H_1 > 0$  for  
 505 the interval  $[T - \epsilon, T]$ , which corresponds to a bang arc  $\alpha = 1$ . ■

506 A control  $\alpha = 1$  implies a strategy in which all resources are allocated to ribosome synthe-  
 507 sis, thus favoring the synthesis of proteins. An intuitive interpretation of Lemma 5.1 is that,  
 508 when approaching the final time  $T$ , the most efficient strategy is to exploit as much as possible  
 509 the available precursors. This is achieved by maximizing the proteins catalyzing  $v_R$ , at the  
 510 expense of arresting the uptake of nutrients  $v_M$  from the environment. In order to further  
 511 describe the optimal control, we can analyze the singular extremals. A singular arc occurs  
 512 when the switching function  $H_1$  vanishes over a subinterval of time. A detailed description  
 513 of the singular arcs can be done by differentiating succesively the switching function  $H_1$  until  
 514 the singular control  $\alpha_{\text{sing}}$  can be obtained as a function of the state  $\varphi$  and the adjoint state  $\lambda$ .

### 515 5.3. Study of the singular arcs.

516 **5.3.1. Introduction.** We assume  $H_1$  vanishes on a whole sub-interval  $[t_1, t_2] \subset [0, T]$ , so  
 517 the extremal belongs to the singular surface

$$518 \quad \Sigma \doteq \{(\varphi, \lambda) \in \mathbb{R}^6 : H_1(\varphi, \lambda) = 0\}.$$

520 Since  $H_1$  vanishes identically, so does its derivative with respect to time. Differentiating along  
 521 an extremal  $(\varphi, \lambda)$  amounts to taking a Poisson bracket<sup>3</sup> with the Hamiltonian  $H$  [28]. Indeed,  
 522 along the singular arc,

$$523 \quad 0 = \dot{H}_1 = \frac{\partial H_1}{\partial \varphi} \dot{\varphi} + \frac{\partial H_1}{\partial \lambda} \dot{\lambda} = \sum_{i=1}^n \left( \frac{\partial H}{\partial \lambda_i} \frac{\partial H_1}{\partial \varphi_i} - \frac{\partial H}{\partial \varphi_i} \frac{\partial H_1}{\partial \lambda_i} \right) = \{H, H_1\} = \{H_0, H_1\}.$$

524 The first derivative  $\dot{H}_1 = H_{01} \doteq \{H_0, H_1\}$  is equal to  $\langle \lambda, F_{01} \rangle$ , where  $F_{01}$  corresponds to the  
 525 Lie bracket of the vector fields  $F_0$  and  $F_1$ . Differentiating again we obtain

$$526 \quad 0 = \dot{H}_{01} = H_{001} + \alpha H_{101}.$$

527 Again,  $H_{001} \doteq \langle \lambda, F_{001} \rangle$  where, with the same notation as before,  $F_{001}$  is the Lie bracket of  $F_0$   
 528 with  $F_{01}$ . If, on the set

$$529 \quad \Sigma' \doteq \{(\varphi, \lambda) \in \mathbb{R}^6 : H_1(\varphi, \lambda) = H_{01}(\varphi, \lambda) = 0\},$$

530 the bracket  $H_{101}$  is also zero, the control disappears from the previous equality, and one has  
 531 to differentiate at least two more times to retrieve the control:  $H_{0001}$  is also zero, and

$$532 \quad (5.4) \quad 0 = H_{00001} + \alpha H_{10001}.$$

533 If the length-five bracket  $H_{10001}$  is not zero, the singular arc is of *order two*. When  $H_{101}$   
 534 vanishes not only on  $\Sigma'$  but on all  $\mathbb{R}^6$ , the order is said to be *intrinsic* and connections  
 535 between bang and singular arcs can only occur through an infinite number of switchings [29],  
 536 the so-called Fuller phenomenon. Otherwise, the order is termed *local*, and Fuller phenomenon  
 537 may or may not occur. Using (5.4), the singular control  $u_s$  is obtained as a function of both  
 538 the state  $\varphi$  and the adjoint state  $\lambda$  as

$$539 \quad \alpha_s(\varphi, \lambda) \doteq -\frac{H_{00001}}{H_{10001}}.$$

540 In our low-dimensional situation, there exists the possibility that the singular control is in  
 541 feedback form, that is, as a function of the state only. The latter can be verified by rewriting  
 542 the system in dimension four (Mayer optimal control formulation where the final volume is

---

<sup>3</sup>The poisson bracket  $\{f, g\}$  of two functions  $f$  and  $g$  along an extremal  $(\varphi, \lambda)$  is defined as

$$\{f, g\} = \sum_{i=1}^n \left( \frac{\partial f}{\partial \lambda_i} \frac{\partial g}{\partial \varphi_i} - \frac{\partial f}{\partial \varphi_i} \frac{\partial g}{\partial \lambda_i} \right).$$

543 maximized), in terms of  $\tilde{\varphi} \doteq (p, r, m, \mathcal{V})$  and its adjoint  $\tilde{\lambda} \doteq (\lambda_p, \lambda_r, \lambda_m, \lambda_{\mathcal{V}})$ . The dynamics is  
 544 affine in the control,

$$545 \quad \dot{\tilde{\varphi}} = \tilde{F}_0(\tilde{\varphi}) + \alpha \tilde{F}_1(\tilde{\varphi}),$$

546 and so is the Hamiltonian:

$$547 \quad \tilde{H}(\tilde{\varphi}, \tilde{\lambda}, \alpha) = \tilde{H}_0 + \alpha \tilde{H}_1,$$

548 with  $\tilde{H}_i = \langle \tilde{\lambda}, \tilde{F}_i \rangle$ ,  $i = 0, 1$ . The same computation as before leads to the following relations  
 549 along a singular arc of order two:

$$550 \quad 0 = \dot{\tilde{H}}_1 = \dot{\tilde{H}}_{01} = \dot{\tilde{H}}_{001} = \dot{\tilde{H}}_{0001},$$

551 and

$$552 \quad 0 = \tilde{H}_{00001} + \alpha \tilde{H}_{10001}.$$

553 **Proposition 5.2.** *Assume that, for all  $\varphi$ ,  $\tilde{F}_1$ ,  $\tilde{F}_{01}$ , and  $\tilde{F}_{001}$  are independent. Then, an*  
 554 *order two singular control depends only on the state  $\tilde{\varphi}$ , and can be expressed as*

$$555 \quad \alpha_s(\tilde{\varphi}) = - \frac{\det \left( \tilde{F}_1, \tilde{F}_{01}, \tilde{F}_{001}, \tilde{F}_{00001} \right)}{\det \left( \tilde{F}_1, \tilde{F}_{01}, \tilde{F}_{001}, \tilde{F}_{10001} \right)}.$$

556 *Proof.* The previous relations imply that  $\tilde{\lambda}$  is orthogonal to  $\tilde{F}_1$ ,  $\tilde{F}_{01}$ ,  $\tilde{F}_{001}$ , and also to  
 557  $\tilde{F}_{00001} + \alpha \tilde{F}_{10001}$ . If these four vector fields were independent at some point along the singular  
 558 arc,  $\tilde{\lambda} \in \mathbb{R}^4$  would vanish: for a problem in Mayer form, this would contradict the maximum  
 559 principle. So their determinant must vanish everywhere along the arc and

$$560 \quad \det \left( \tilde{F}_1, \tilde{F}_{01}, \tilde{F}_{001}, \tilde{F}_{00001} \right) + \alpha \det \left( \tilde{F}_1, \tilde{F}_{01}, \tilde{F}_{001}, \tilde{F}_{10001} \right) = 0.$$

561 If the second determinant was zero, given the rank assumption on the first three vector fields,  
 562  $\tilde{F}_{10001}$  would belong to their span; but this is impossible since it would imply  $H_{10001} = 0$ ,  
 563 contradicting the fact that the singular is of order two. ■

564 Going back to the three-dimensional formulation, one can explicit the computations by  
 565 successively differentiating the expression (5.3).

566 **5.3.2. Singular arc in feedback form.** The condition  $H_1 = 0$  could be a consequence of  
 567 the growth rate  $w_R(p)(r - r_{\min})$  vanishing over the whole interval  $[t_1, t_2]$ . We will see this is  
 568 not possible given the dynamics of the system.

569 **Proposition 5.3.** *The growth rate  $\mu(p, r) = w_R(p)(r - r_{\min})$  cannot vanish along the optimal*  
 570 *solution of (OCP).*

571 *Proof.* For any trajectory of (S') with initial conditions (IC), control  $\alpha(\cdot) \in \mathcal{U}$  and  
 572  $t \in [0, T]$ , we have  $\dot{p} \leq E_M r_{\max}$ , which means  $p \leq p_{\max}^T \doteq E_M r_{\max} T + p(0)$ . Then,

573  $\dot{r} \geq -r_{\max} w_R(p_{\max}^T)(r - r_{\min})$ . Additionally, since  $w_R(p)$  is continuously differentiable, there  
 574 exists  $c$  such that  $cp \geq w_R(p)$ , which means that  $\dot{p} \geq -cp(p_{\max}^T + 1)(r_{\max} - r_{\min})$ . Then,  
 575 at worst, the state  $p$  (respectively,  $r$ ) decays exponentially towards the value 0 (respectively,  
 576  $r_{\min}$ ), which cannot be attained in finite time. ■

577 As a consequence of Proposition 5.3, the condition  $H_1 = 0$  becomes

$$578 \text{ (Condition 1)} \quad \lambda_r - \lambda_m = 0.$$

580 We define the quantity  $\phi(\varphi, \lambda) \doteq (r_{\max} - m - r)\lambda_r - (p + 1)\lambda_p - \lambda^0$ , so that the time derivative  
 581 of (Condition 1) is

$$582 \text{ (Condition 2)} \quad \phi(\varphi, \lambda)w_R(p) - E_M\lambda_p = 0.$$

584 Along a singular arc, the Hamiltonian can be rewritten as

$$585 \text{ (5.5)} \quad H = E_M m \lambda_p + \phi(\varphi, \lambda)w_R(p)(r - r_{\min}),$$

587 and, using (Condition 1) and (Condition 2), the adjoint system becomes

$$588 \quad \begin{cases} \frac{d\lambda_p}{dt} = w_R(p)(r - r_{\min})\lambda_p - \phi(\varphi, \lambda)w'_R(p)(r - r_{\min}), \\ \frac{d\lambda_r}{dt} = w_R(p)(r - r_{\min})\lambda_r - \phi(\varphi, \lambda)w_R(p). \end{cases}$$

589

590 **Proposition 5.4.** *Neither  $\phi(\varphi, \lambda)$  nor  $\lambda_p$  can vanish along a singular arc.*

591 *Proof.* According to (Condition 2), if either  $\phi(\varphi, \lambda)$  or  $\lambda_p$  are null, then both of them are  
 592 null. Then, if  $\phi(\varphi, \lambda) = \lambda_p = 0$ , equation (5.5) would imply that the Hamiltonian vanishes  
 593 in  $\Sigma$ , and therefore it would vanish for the whole interval  $[0, T]$  (as it is constant along the  
 594 solution). However, one can see in (5.1) that the Hamiltonian evaluated at final time is  
 595  $-\lambda^0 w_R(p(T))(r(T) - r_{\min})$  which cannot be 0 due to Proposition 5.3 and  $\lambda^0 \neq 0$ . ■

596 We differentiate (Condition 2) w.r.t. time and we get  $\dot{\phi}(\varphi, \lambda)w_R(p) + \phi(\varphi, \lambda)w'_R(p)\dot{p} - E_M\dot{\lambda}_p$   
 597  $= 0$ . Replacing the latter and using Proposition 5.4 allows us to reduce the expression to

$$598 \text{ (Condition 3)} \quad -(r_{\max} - r_{\min})w_R(p)^2 + E_M(m + r - r_{\min})w'_R(p) = 0,$$

600 which allows us to express  $m + r$  in terms of  $p$ .

601 **Lemma 5.5.** *Along a singular arc over the interval  $[t_1, t_2]$ ,*

$$602 \quad m + r = x(p)$$

604 *with  $x(p) : \mathbb{R}_+ \rightarrow [r_{\min}, \infty)$  defined as*

$$605 \quad x(p) \doteq (r_{\max} - r_{\min}) \frac{w_R(p)^2}{E_M w'_R(p)} + r_{\min},$$

606

607 *which, using (3.7), yields  $x(p_{\text{opt}}^*) = r_{\max}$ .*

608 The fact that the control does not show up in (Condition 3)—which is obtained by differentiat-  
 609 ing (Condition 1) twice—means that the singular arc is *at least* of order two. We differentiate  
 610 (Condition 3) and we get

$$611 \text{ (Condition 4)} \quad \left( r_{\max} - x(p) + (p+1)x'(p) \right) w_R(p)(r - r_{\min}) - E_M m x'(p) = 0.$$

613 We define the function

$$614 \text{ (5.6)} \quad y(p) \doteq w_R(p) \left( r_{\max} - x(p) + (p+1)x'(p) \right).$$

616 Using (Condition 3) and (5.6) in (Condition 4) yields

$$617 \quad (x(p) - r_{\min})y(p) - \left( E_M x'(p) + y(p) \right) m = 0,$$

619 which means we can express  $m$  and  $r$  in terms of  $p$  along the singular arc.

620 **Lemma 5.6.** *Along a singular arc over the interval  $[t_1, t_2]$ ,*

$$621 \text{ (5.7)} \quad m = (x(p) - r_{\min}) \frac{y(p)}{E_M x'(p) + y(p)},$$

$$622 \text{ (5.8)} \quad r = x(p) - (x(p) - r_{\min}) \frac{y(p)}{E_M x'(p) + y(p)}.$$

624 We differentiate (Condition 4) and we get

$$625 \text{ (5.9)} \quad - (r_{\max}(1 - \alpha) - m) w_R(p)(r - r_{\min}) + x'(p) \frac{y(p)}{E_M x'(p) + y(p)} \dot{p} \\ 626 + (x(p) - r_{\min}) \left( \frac{y'(p)}{E_M x'(p) + y(p)} - \frac{y(p)}{(E_M x'(p) + y(p))^2} (E_M x''(p) + y'(p)) \right) \dot{p} = 0,$$

627 meaning that we can express

$$628 \quad \alpha_{\text{sing}}(p) = 1 - \frac{m}{r_{\max}} \left( \left( \frac{x'(p)}{x(p) - r_{\min}} + \frac{y'(p)}{y(p)} - \frac{E_M x''(p) + y'(p)}{E_M x'(p) + y(p)} \right) \frac{\dot{p}}{w_R(p)(r - r_{\min})} + 1 \right).$$

630 While (Condition 3) showed that the order of the singular arc is *at least* two, the latter relation  
 631 proves that it is *exactly* two. Indeed, the coefficient before  $\alpha$  in (5.9) is  $-r_{\max} w_R(p)(r - r_{\min})$ ,  
 632 which cannot vanish as proven in Proposition 5.3. The singular arc is said to be *locally of order*  
 633 *two*, as the coefficient of  $\alpha$  in (Condition 3) is zero along the singular arc, but not everywhere  
 634 on the cotangent bundle [29]. In this case, the presence of the Fuller phenomenon (i.e. the  
 635 junctions between bang and singular arcs constituting an infinite number of switchings) is  
 636 not guaranteed. However, this turns out to be the case as it will be shown in the numerical  
 637 computations. Besides, in accordance with Proposition 5.2, the order two singular control  
 638 can be expressed in feedback form, i.e. as a function of the state only. Using a numerical  
 639 rank test (e.g. Singular Value Decomposition), we verified that the rank condition is fulfilled.  
 640 More precisely, the actual computation proves that the singular control can be expressed as a  
 641 function of  $p$  only (Lemma 5.6 entails that  $r$ ,  $m$  and therefore  $\dot{p}$  can be expressed in terms of  
 642  $p$ ), which allows to retrieve the turnpike behaviour as described in the following section.

643 **5.3.3. The turnpike phenomenon.** Using (5.7) and (5.8), we see that the dynamical  
644 equation of  $p$  becomes

$$645 \quad \dot{p} = E_M w_R(p) \frac{x(p) - r_{\min}}{E_M x'(p) + y(p)} (r_{\max} - x(p)),$$

647 which is only equal to 0 when  $r_{\max} = x(p)$ . This is only true at  $p = p_{\text{opt}}^*$ , and so

$$648 \quad \text{sign}(\dot{p}) = \text{sign}(p_{\text{opt}}^* - p),$$

650 meaning that, in a singular arc over the interval  $[t_1, t_2]$ , the concentration  $p$  converges asymp-  
651 totically to the optimal value  $p_{\text{opt}}^*$ . This means that  $m$  and  $r$  would also converge to the optimal  
652 values  $m_{\text{opt}}^*$  and  $r_{\text{opt}}^*$ , respectively, and the singular control  $\alpha_{\text{sing}}$  to  $\alpha_{\text{opt}}^*$ . We formalize this  
653 in the following theorem.

654 **Theorem 5.7.** *On a singular arc, the system states and singular control tend asymptotically*  
655 *to*

$$656 \quad (p, r, m) = (p_{\text{opt}}^*, r_{\text{opt}}^*, m_{\text{opt}}^*),$$

$$657 \quad \alpha_{\text{sing}}(t) = \alpha_{\text{opt}}^*.$$

659 The above theorem is an explicit proof of the presence of the turnpike property: an opti-  
660 mal control characterized by a singular arc that stays exponentially close to the steady-state  
661 solution of the static optimal control problem [30]. This phenomenon has been considerably  
662 studied in econometry [31], and more recently in biology [32, 10, 20]. It has been shown that,  
663 for large final times, the trajectory of the system spends most of the time near the optimal  
664 steady state, and that in infinite horizon problems, it converges to this state.

665 **5.4. Numerical simulations.** The simulations were performed with Bocop [33], which  
666 solves the optimal control problem through a direct method. An online version of the numerical  
667 computations can be visualized and executed on the gallery of the `ct` (Control Toolbox)  
668 project<sup>4</sup>. The time discretization algorithm used is Lobato IIC (implicit, 4-stage, order  
669 6) with 2000 time steps. Figure 3 shows an optimal trajectory with  $r(0) + m(0) < r_{\max}$ ,  
670 where most of the bacterial mass corresponds to class  $Q$  proteins. The obtained optimal  
671 control confirms the conclusions of the latter section: a large part of the time, the optimal  
672 control remains near the optimal steady-state allocation  $\alpha_{\text{opt}}^*$ , according to the turnpike theory  
673 (Theorem 5.7). The solution presents chattering after and before the singular arc (even if  
674 only a finite number of bangs is computed by the numerical method), and the final bang  
675 corresponds to  $\alpha = 1$  (Lemma 5.1). In order to verify the optimality of the singular arc, we  
676 performed a numerical computation of the derivatives of  $H_1$ . The fact that the factor of  $\alpha$  in  
677 the fourth derivative is different from 0 confirms that the singular arc is of order 2. Moreover,  
678 its negativity complies with the *generalized Legendre-Clebsch* condition given by

$$679 \quad (5.10) \quad (-1)^k \frac{\partial}{\partial \alpha} \left( \frac{d^{2k}}{dt^{2k}} H_1 \right) < 0,$$

---

<sup>4</sup><https://ct.gitlabpages.inria.fr/gallery/bacteria/bacteria.html>

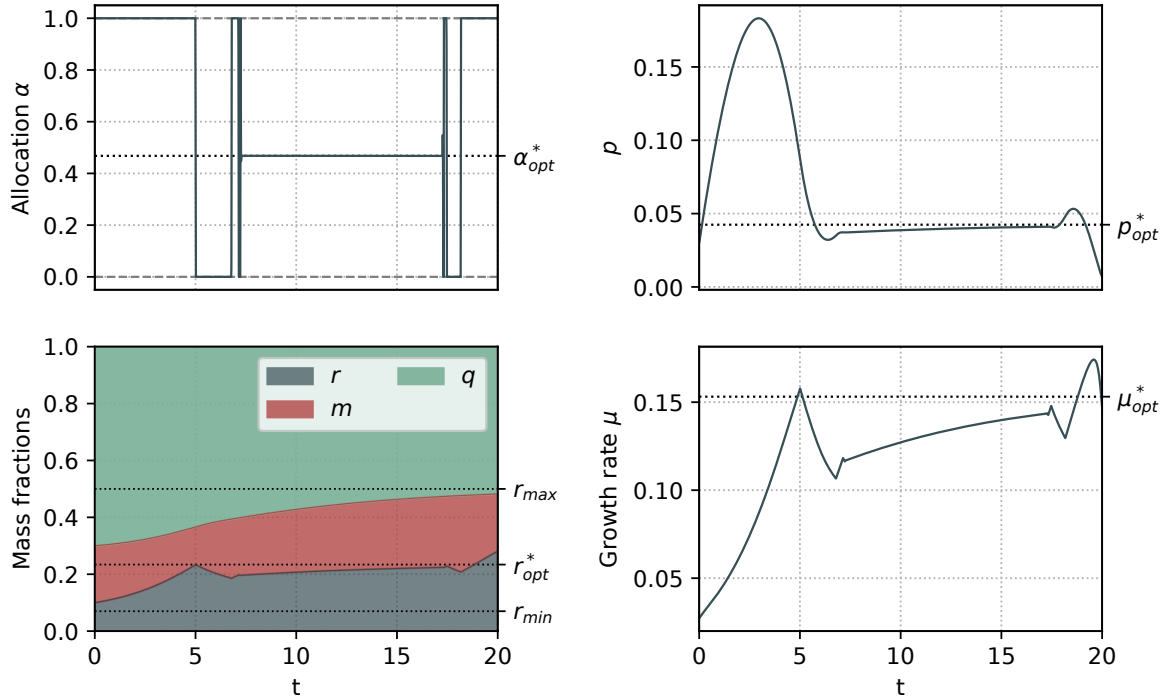


Figure 3: Numerical simulation of (OCP) obtained with Bocop, for the parameter values derived in Section 4. Initial state is  $p(0) = 0.03$ ,  $r(0) = 0.1$ ,  $m(0) = 0.2$  with  $E_M = 0.6$ . As predicted, the optimal control  $\alpha$  involves chattering after and before the singular arc. The mass fraction  $q$  converges to  $1 - r_{max}$  and  $m + r$  to  $r_{max}$ . Moreover, along the singular arc, the states  $(p^*, r^*, m^*)$  converge asymptotically to  $(p_{opt}^*, r_{opt}^*, m_{opt}^*)$ .

681 along the singular arc, which is a necessary condition for optimality. As we state in [23], even  
 682 if there exist no available sufficient condition to verify local optimality of extremals with Fuller  
 683 arcs, a check of the Legendre-Clebsch condition along the singular arc can ensure that the  
 684 extremal obtained is not a too crude local minimizer. For the second-order singular arc case,  
 685 the condition corresponds to the case  $k = 2$ . The initial conditions used in Figure 3 were only  
 686 chosen to confirm the theoretical results found throughout this section, by emphasizing the  
 687 main features of the solution. However, from a biological perspective, a situation where  $r + m$   
 688 is significantly different from its steady-state value  $r_{max}$  is not to be expected: a common  
 689 assumption in these classes of coarse-grained models is that the transcription of Q proteins  
 690 is autoregulated around stable levels [34], which translates into a constant  $q = 1 - r_{max}$  (and  
 691 therefore  $m + r = r_{max}$ ) for the whole interval  $[0, T]$ . We will see in next section that this  
 692 hypothesis produces a very particular structure of the optimal control solution.

693 **6. Biologically relevant scenarios.** Despite their simplicity, self-replicator models have  
 694 been capable of accounting for a number of observable phenomena during steady-state mi-  
 695 crobial growth, under the assumption that bacteria allocate their resources in such a way

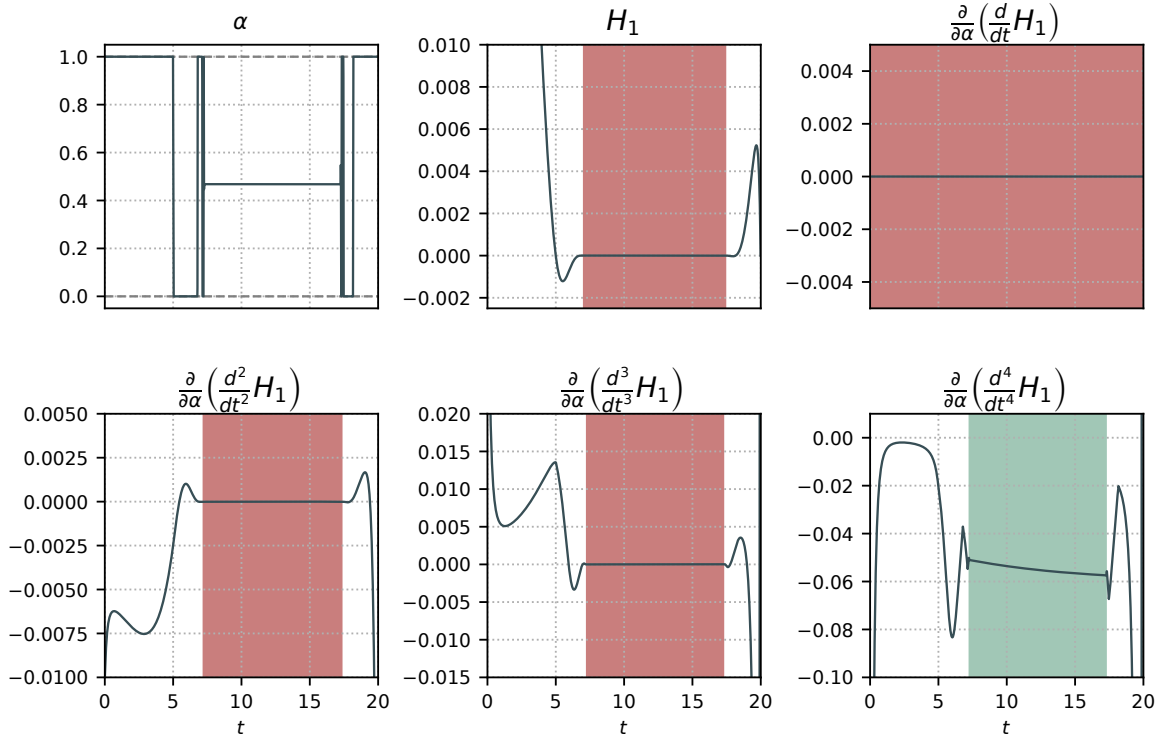


Figure 4: Factors of  $\alpha$  in the derivatives of  $H_1$  evaluated over the trajectory plotted in Figure 3. The intervals where the functions vanish are marked in red. As expected, all functions vanish along the singular arc except for the factor in the fourth derivative (highlighted in green) which is negative according to the Legendre-Clebsch condition (5.10).

696 as to maximize growth. Here, we apply the general optimal allocation strategy derived in  
 697 the previous section to predict the bacterial response to certain environmental changes. We  
 698 consider two situations that commonly affect bacteria: changes in the nutrient concentration  
 699 in the medium, and changes in the environment submitting the cell to a particular stress.

700 **6.1. Nutrient shift.** Bacteria are known to traverse different habitats throughout their  
 701 lifetime, experiencing fluctuating nutrient concentrations in the medium. In [10], we explored  
 702 how bacteria dynamically adjust their allocation strategy when facing a nutrient upshift. In  
 703 this work, we show that considering a class of growth rate-independent proteins in the model  
 704 refines these previous results. We consider the optimal control problem with the initial state  
 705 being the optimal steady state for a low value of  $E_M$ , and we set a higher  $E_M$  for the time  
 706 interval  $[0, T]$ , representing a richer medium. Setting initial conditions at steady state has an  
 707 impact on the singular arc of the optimal control: it holds that  $m + r = r_{\max}$  and  $q = 1 - r_{\max}$   
 708 for the whole trajectory, which yields a constant singular arc.

709 **Theorem 6.1.** *If  $r(0) + m(0) = r_{\max}$  (i.e.,  $q$  starts from a steady-state value), then any*  
 710 *singular arc over the interval  $[t_1, t_2]$  of the optimal control corresponds to the optimal steady*



711 *state.*

712 *Proof.* The dynamical equation for  $q$  is  $\dot{q} = ((1 - r_{\max}) - q)w_R(p)(r - r_{\min})$ , where it can  
 713 be seen that the set  $q = 1 - r_{\max}$  is invariant. This means that, for any trajectory emanating  
 714 from a steady state,  $q$  remains constant even under changes of the nutrient quality  $E_M$ . Then,  
 715 by using the relation (2.5), we obtain

$$716 \quad (6.1) \quad m + r = r_{\max}.$$

718 Along the singular arc, it holds that  $m + r = x(p)$ , which, using (6.1), implies that  $p = p_{\text{opt}}^*$ ,  
 719 meaning that the precursor concentration along the singular arc is constant and optimal.  
 720 Then,  $\alpha_{\text{sing}} = \alpha_{\text{opt}}^*$ ,  $m = m_{\text{opt}}^*$  and  $r = r_{\text{opt}}^*$  for the whole singular arc. ■

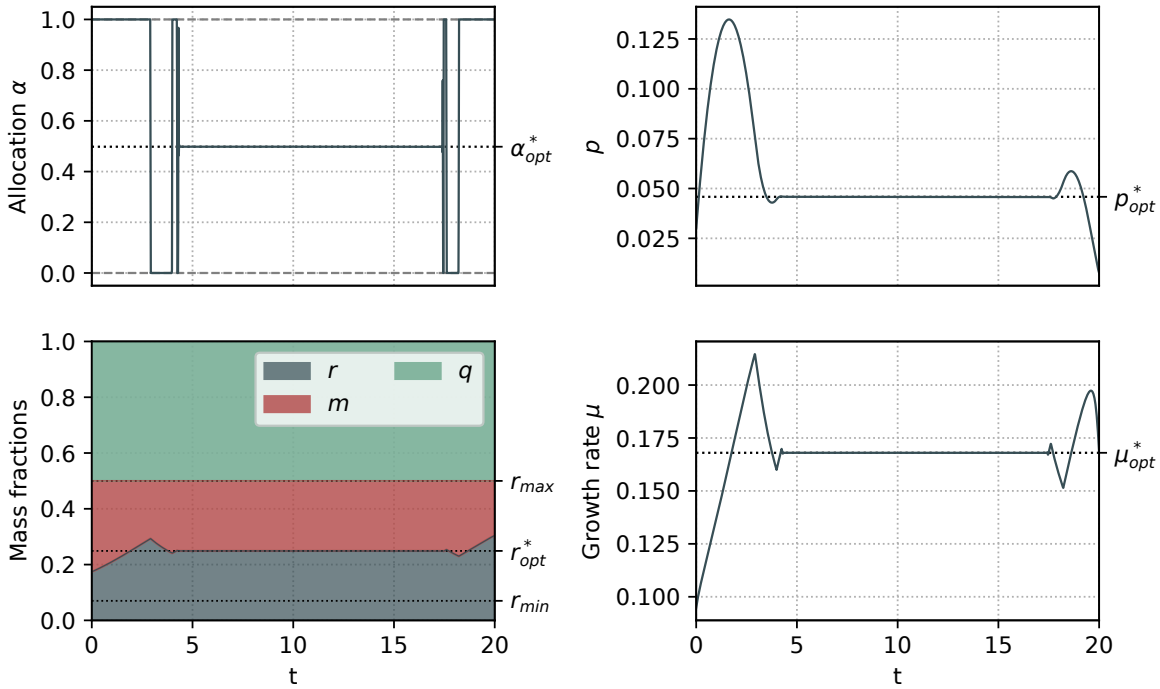


Figure 5: Numerical simulation of the optimal control problem starting from a steady state. The initial state corresponds to the optimal steady state for  $E_M = 0.3$  (poor medium), and the new environmental constant is fixed to  $E_M = 0.7$  (rich medium). As predicted,  $m + r$  ( $= 1 - q$ ) remains constant, even if they vary individually, in opposition to the previous case. Naturally, an increase in the nutrient quality produces a higher steady-state ribosomal mass fraction  $r^*$ , which yields an increased steady-state growth rate  $\mu_{\text{opt}}^*$  with respect to the growth rate before the upshift.

721 A numerical simulation of this scenario is shown in Figure 5. As expected, the increase  
 722 in  $E_M$  produces a higher ribosomal mass fraction  $r$ , which translates into an increase of the  
 723 growth rate, stabilizing at the maximal steady-state growth rate  $\mu_{\text{opt}}^*$  through an oscillatory

724 phase. It is noteworthy that, in comparison to Giordano *et al.*'s model, the relative changes  
 725 in mass fractions  $r$  and  $m$  are much lower, which corresponds well with the relative changes  
 726 observed in [6]. Additionally, while the presence of  $r_{\min}$  does not noticeably affect the solution  
 727 of the optimal control problem, it contributes to a model that more accurately reproduces the  
 728 experimental data (Figure 2a), representing a significant improvement from the modeling  
 729 point of view.

730 **6.2. Bacterial response to stress.** The other scenario of interest is an environmental  
 731 change imposing a certain stress on the microbial population, which is counteracted through  
 732 the synthesis of a stress response protein W. This protein is also growth rate-independent like  
 733 Q, and its production can be triggered by many different situations. For instance, when subject  
 734 to extreme temperatures, the production of so-called molecular chaperones helps bacteria  
 735 counter the effect of protein unfolding [35, 14]. Likewise, the production of other proteins is  
 736 known to protect bacteria like *E. coli* against acid stress [36]. Another possible scenario is the  
 737 response to metabolic load imposed by the induced overexpression of a heterologous protein  
 738 [37]. All of these situations are known to reduce the resources available for growth-associated  
 739 proteins (Figure 6), consequently decreasing the maximal growth rate attainable. Here, we  
 740 model a general stress response through the production of the W protein that takes up a  
 741 fraction  $w$  of the proteome, thus reducing  $r_{\max}$  to a certain  $r_{\max}^w < r_{\max}$ .

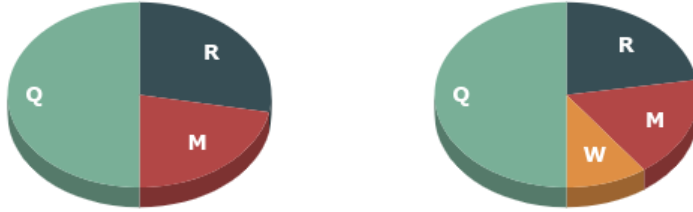


Figure 6: Left: original case. Right: new proposed case, where  $q$  remains unchanged, but the maximal allocation  $m + r$  is restricted to a  $r_{\max}^w < r_{\max}$ .

742 As before, we assume  $q$  takes up a constant fraction  $1 - r_{\max}$  of the proteome, but the  
 743 proportions of resources allocated to M and R are now  $r_{\max}^w \alpha$  and  $r_{\max}^w (1 - \alpha)$  respectively.  
 744 By construction, we have  $w = r_{\max} - m - r$ , which means we can express

$$745 \dot{w} = (r_{\max} - r_{\max}^w - w)w_R(p)(r - r_{\min}),$$

747 showing that the mass fraction  $w$  converges asymptotically to the difference  $r_{\max} - r_{\max}^w$ . The  
 748 remaining mass fractions  $p$ ,  $r$  and  $m$  obey the dynamics of system (S'), so the application of  
 749 the optimal solution found in last section is straightforward. An example is shown in Figure  
 750 7. As predicted,  $m + r$  converges to the reduced  $r_{\max}^w$ ,  $q$  remains constant at  $1 - r_{\max}$  and  $w$   
 751 converges to  $r_{\max}^w - r_{\max}$ . The reduction of resources available for growth-associated proteins  
 752 (M and R) causes the growth rate to drop, as was shown experimentally [6].

753 **7. Discussion.** In this work, we proposed a dynamical self-replicator model of bacterial  
 754 growth based on the work of [10], which introduces a growth rate-independent class of pro-

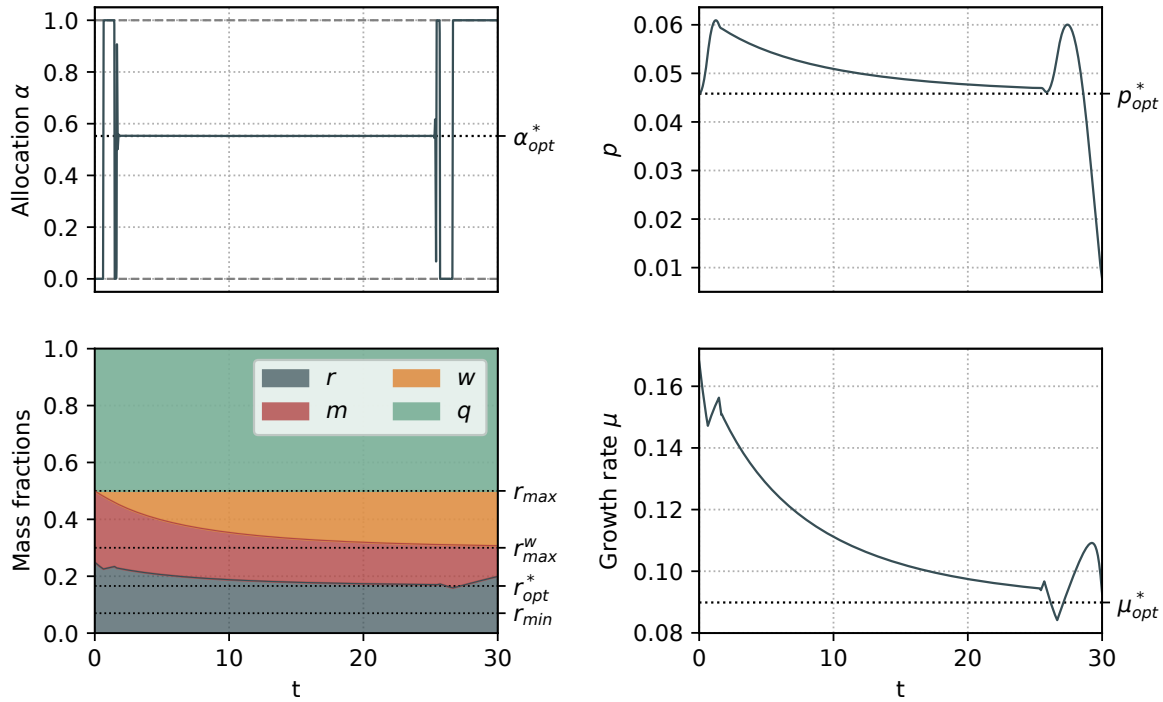


Figure 7: Numerical simulation of an optimal trajectory where the initial conditions are the optimal steady state for  $E_M = 0.7$  and  $r_{\max} = 0.5$ . A certain stress is induced at  $t = 0$ , which triggers the synthesis of the growth rate-independent protein  $w$ , reducing the fraction  $r_{\max}$  to  $r_{\max}^w = 0.3$ . As a result, the steady-state growth rate is significantly reduced.

755 tein. As a consequence, the proteome of the bacterial cell can be divided into the metabolic  
 756 machinery M, the gene expression machinery R, and the housekeeping machinery Q. While Q  
 757 is growth rate-independent, this is also the case for a fraction of R required for cell replication  
 758 to occur. As a consequence of this hypothesis, a maximum ribosomal concentration  $r_{\max}$  ap-  
 759 pears in the model kinetics, limiting the allocation of resources to M and R. We studied the  
 760 asymptotic behavior of the system, showing that, under certain conditions, all solutions con-  
 761 verge towards the only globally attractive equilibrium. We then explored the optimal dynamic  
 762 allocation strategies that consider maximizing the bacterial population volume in terms of the  
 763 resource allocation parameter  $\alpha$ . This involved a study of the static and dynamic aspects  
 764 of optimal strategies. For the first one, we showed there is a unique optimal steady state,  
 765 which corresponds to experimental observations of growing cultures of *E. coli* [26, 27, 6, 24].  
 766 The dynamic problem is approached through optimal control theory, by application of the  
 767 Pontrjagin's Maximum Principle. The obtained optimal control has a Fuller-singular-Fuller  
 768 structure with a non-constant singular arc, in contrast to the constant singular arc obtained  
 769 in Giordano *et al.*'s approach. We performed a detailed analysis of the OCP in both analytic  
 770 and numerical ways. In particular, the singular arc of the optimal solution is characterized

771 by i) its feedback form (i.e. being expressed as a function of the state only), ii) being exactly  
772 of order 2, and iii) the turnpike phenomenon (where the state trajectory and optimal control  
773 converge asymptotically towards the optimal steady state and control). Moreover, we showed  
774 that, when the mass fraction of class  $Q$  proteins is at steady state, the singular arc of the  
775 optimal solution corresponds to the optimal steady state. Additionally, we showed that the  
776 dynamical approach can be used to predict the behavior of the system when subject to stress.  
777 The latter is modeled through a reduction of the fraction of growth rate-dependent protein  
778 synthesis as the production of a  $w$  protein that reduces  $r_{\max}$ .

779 While the main features of Giordano *et. al.*'s work are present in this approach, our  
780 generalization shows a better agreement with the experimental data given by the introduc-  
781 tion of the parameters  $r_{\max}$  and  $r_{\min}$  in the model. Additionally, the proposed partition of  
782 the proteome in a dynamic setting can account for certain natural phenomena known to re-  
783 duce the fraction of growth rate-dependent proteins in the cell. These modifications yield  
784 interesting optimal control problems, which could potentially help understand the internal  
785 decision-making mechanisms evolved by bacteria.

786 **Acknowledgments.** We would like to acknowledge the help of S. Psalmon and B. Schall  
787 from **Polytech Nice Sophia** for the numerical simulations.

788

## REFERENCES

- 789 [1] M. SCHAECHTER, J. L. INGRAHAM, AND F. C. NEIDHARDT, *Microbe*, ASM Press, Washington, DC,  
790 2006.
- 791 [2] F. NEIDHARDT, *Bacterial growth: constant obsession with  $dN/dt$* , *J. Bacteriol.*, 181 (1999), pp. 7405–  
792 7408.
- 793 [3] S. BRUL, S. VAN GERWEN, AND M. ZWIETERING, *Modelling Microorganisms in Food*, Elsevier, 2007.
- 794 [4] A. BRAUNER, O. FRIDMAN, O. GEFEN, AND N. Q. BALABAN, *Distinguishing between resistance, toler-*  
795 *ance and persistence to antibiotic treatment*, *Nature Reviews Microbiology*, 14 (2016), pp. 320–330.
- 796 [5] J. C. LIAO, L. MI, S. PONTRELLI, AND S. LUO, *Fuelling the future: microbial engineering for the*  
797 *production of sustainable biofuels*, *Nature Reviews Microbiology*, 14 (2016), pp. 288–304.
- 798 [6] M. SCOTT, C. W. GUNDERSON, E. M. MATEESCU, Z. ZHANG, AND T. HWA, *Interdependence of cell*  
799 *growth and gene expression: origins and consequences*, *Science*, 330 (2010), pp. 1099–1102.
- 800 [7] H. VAN DEN BERG, Y. KISELEV, AND M. ORLOV, *Optimal allocation of building blocks between nutrient*  
801 *uptake systems in a microbe*, *Journal of Mathematical Biology*, 44 (2002), pp. 276–296.
- 802 [8] D. MOLENAAR, R. VAN BERLO, D. DE RIDDER, AND B. TEUSINK, *Shifts in growth strategies reflect*  
803 *tradeoffs in cellular economics*, *Molecular Systems Biology*, 5 (2009), p. 323.
- 804 [9] A. Y. WEISSE, D. A. OYARZÚN, V. DANOS, AND P. S. SWAIN, *Mechanistic links between cellular trade-*  
805 *offs, gene expression, and growth*, *Proceedings of the National Academy of Sciences*, 112 (2015),  
806 pp. E1038–E1047.
- 807 [10] N. GIORDANO, F. MAIRET, J.-L. GOUZÉ, J. GEISELMANN, AND H. DE JONG, *Dynamical allocation*  
808 *of cellular resources as an optimal control problem: novel insights into microbial growth strategies*,  
809 *PLoS computational biology*, 12 (2016), p. e1004802.
- 810 [11] D. W. ERICKSON, S. J. SCHINK, V. PATSALO, J. R. WILLIAMSON, U. GERLAND, AND T. HWA, *A*  
811 *global resource allocation strategy governs growth transition kinetics of Escherichia coli*, *Nature*, 551  
812 (2017), pp. 119–123.
- 813 [12] H. DOURADO AND M. J. LERCHER, *An analytical theory of balanced cellular growth*, *Nature communi-*  
814 *cations*, 11 (2020), pp. 1–14.
- 815 [13] M. SCOTT, S. KLUMPP, E. MATEESCU, AND T. HWA, *Emergence of robust growth laws from optimal*  
816 *regulation of ribosome synthesis*, *Molecular Systems Biology*, 10 (2014), p. 747.
- 817 [14] F. MAIRET, J.-L. GOUZÉ, AND H. DE JONG, *Optimal proteome allocation and the temperature depen-*

- dence of microbial growth laws, npj Systems Biology and Applications, 7 (2021), pp. 1–11.
- [15] M. BASAN, S. HUI, H. OKANO, Z. ZHANG, Y. SHEN, J. WILLIAMSON, AND T. HWA, *Overflow metabolism in Escherichia coli results from efficient proteome allocation*, Nature, 528 (2015), pp. 99–104.
- [16] A. MAITRA AND K. DILL, *Bacterial growth laws reflect the evolutionary importance of energy efficiency*, Proceedings of the National Academy of Sciences of the USA, 112 (2015), pp. 406–411.
- [17] D. A. CARLSON, A. B. HAURIE, AND A. LEIZAROWITZ, *Infinite Horizon Optimal Control*, Springer, Berlin, Heidelberg, 1991.
- [18] I. YEGOROV, F. MAIRET, AND J.-L. GOUZÉ, *Optimal feedback strategies for bacterial growth with degradation, recycling, and effect of temperature*, Optimal Control Applications and Methods, 39 (2018), pp. 1084–1109.
- [19] J. IZARD, C. G. BALDERAS, D. ROPERS, S. LACOUR, X. SONG, Y. YANG, A. LINDNER, J. GEISELMANN, AND H. DE JONG, *A synthetic growth switch based on controlled expression of RNA polymerase*, Molecular Systems Biology, 11 (2015), p. 840.
- [20] I. YEGOROV, F. MAIRET, H. DE JONG, AND J.-L. GOUZÉ, *Optimal control of bacterial growth for the maximization of metabolite production*, Journal of mathematical biology, 78 (2019), pp. 985–1032.
- [21] A. G. YABO, J.-B. CAILLAU, AND J.-L. GOUZÉ, *Singular regimes for the maximization of metabolite production*, in 2019 IEEE 58th Conference on Decision and Control (CDC), IEEE, 2019, pp. 31–36.
- [22] A. G. YABO AND J.-L. GOUZÉ, *Optimizing bacterial resource allocation: metabolite production in continuous bioreactors*, in IFAC World Congress 2020, 2020.
- [23] A. G. YABO, J.-B. CAILLAU, AND J.-L. GOUZÉ, *Optimal bacterial resource allocation: metabolite production in continuous bioreactors*, Mathematical Biosciences and Engineering, 17 (2020), pp. 7074–7100.
- [24] S. HUI, J. M. SILVERMAN, S. S. CHEN, D. W. ERICKSON, M. BASAN, J. WANG, T. HWA, AND J. R. WILLIAMSON, *Quantitative proteomic analysis reveals a simple strategy of global resource allocation in bacteria*, Molecular systems biology, 11 (2015), p. 784.
- [25] M. BASAN, M. ZHU, X. DAI, M. WARREN, D. SÉVIN, Y.-P. WANG, AND T. HWA, *Inflating bacterial cells by increased protein synthesis*, Molecular systems biology, 11 (2015), p. 836.
- [26] J. FORCHHAMMER AND L. LINDAHL, *Growth rate of polypeptide chains as a function of the cell growth rate in a mutant of Escherichia coli 15*, Journal of molecular biology, 55 (1971), pp. 563–568.
- [27] H. BREMER, P. P. DENNIS, ET AL., *Modulation of chemical composition and other parameters of the cell by growth rate*, Escherichia coli and Salmonella: cellular and molecular biology, 2 (1996), pp. 1553–69.
- [28] A. A. AGRACHEV AND Y. SACHKOV, *Control Theory from the Geometric Viewpoint*, vol. 87, Springer Science & Business Media, 2013.
- [29] M. I. ZELIKIN AND V. F. BORISOV, *Theory of Chattering Control: with Applications to Astronautics, Robotics, Economics, and Engineering*, Springer Science & Business Media, 2012.
- [30] E. TRÉLAT AND E. ZUAZUA, *The turnpike property in finite-dimensional nonlinear optimal control*, Journal of Differential Equations, 258 (2015), pp. 81–114.
- [31] D. CASS, *Optimum growth in an aggregative model of capital accumulation*, The Review of economic studies, 32 (1965), pp. 233–240.
- [32] J.-M. CORON, P. GABRIEL, AND P. SHANG, *Optimization of an amplification protocol for misfolded proteins by using relaxed control*, Journal of mathematical biology, 70 (2015), pp. 289–327.
- [33] I. S. TEAM COMMANDS, *BOCOP: an open source toolbox for optimal control*. <http://bocop.org>, 2017.
- [34] S. KLUMPP, Z. ZHANG, AND T. HWA, *Growth rate-dependent global effects on gene expression in bacteria*, Cell, 139 (2009), pp. 1366–1375.
- [35] D. RONCARATI AND V. SCARLATO, *Regulation of heat-shock genes in bacteria: from signal sensing to gene expression output*, FEMS microbiology reviews, 41 (2017), pp. 549–574.
- [36] N. GUAN AND L. LIU, *Microbial response to acid stress: mechanisms and applications*, Applied microbiology and biotechnology, 104 (2020), pp. 51–65.
- [37] H. DONG, L. NILSSON, AND C. G. KURLAND, *Gratuitous overexpression of genes in Escherichia coli leads to growth inhibition and ribosome destruction.*, Journal of bacteriology, 177 (1995), pp. 1497–1504.